Technical Report IRRP-97-3
April 1997

US Army Corps of Engineers
Waterways Experiment Station

Installation Restoration Research Program

Simplified Concepts in Spectroscopy and Photochemistry

by Mohammed Qasim

Approved For Public Release; Distribution Is Unlimited

Prepared for Headquarters, U.S. Army Corps of Engineers

Installation Restoration Research Program

Technical Report IRRP-97-3
April 1997

Simplified Concepts in Spectroscopy and Photochemistry

by Mohammed Qasim

U.S. Army Corps of Engineers
Waterways Experiment Station
3909 Halls Ferry Road
Vicksburg, MS 39180-6199

Final report

Approved for public release; distribution is unlimited

Prepared for U.S. Army Corps of Engineers
Washington, DC 20314-1000

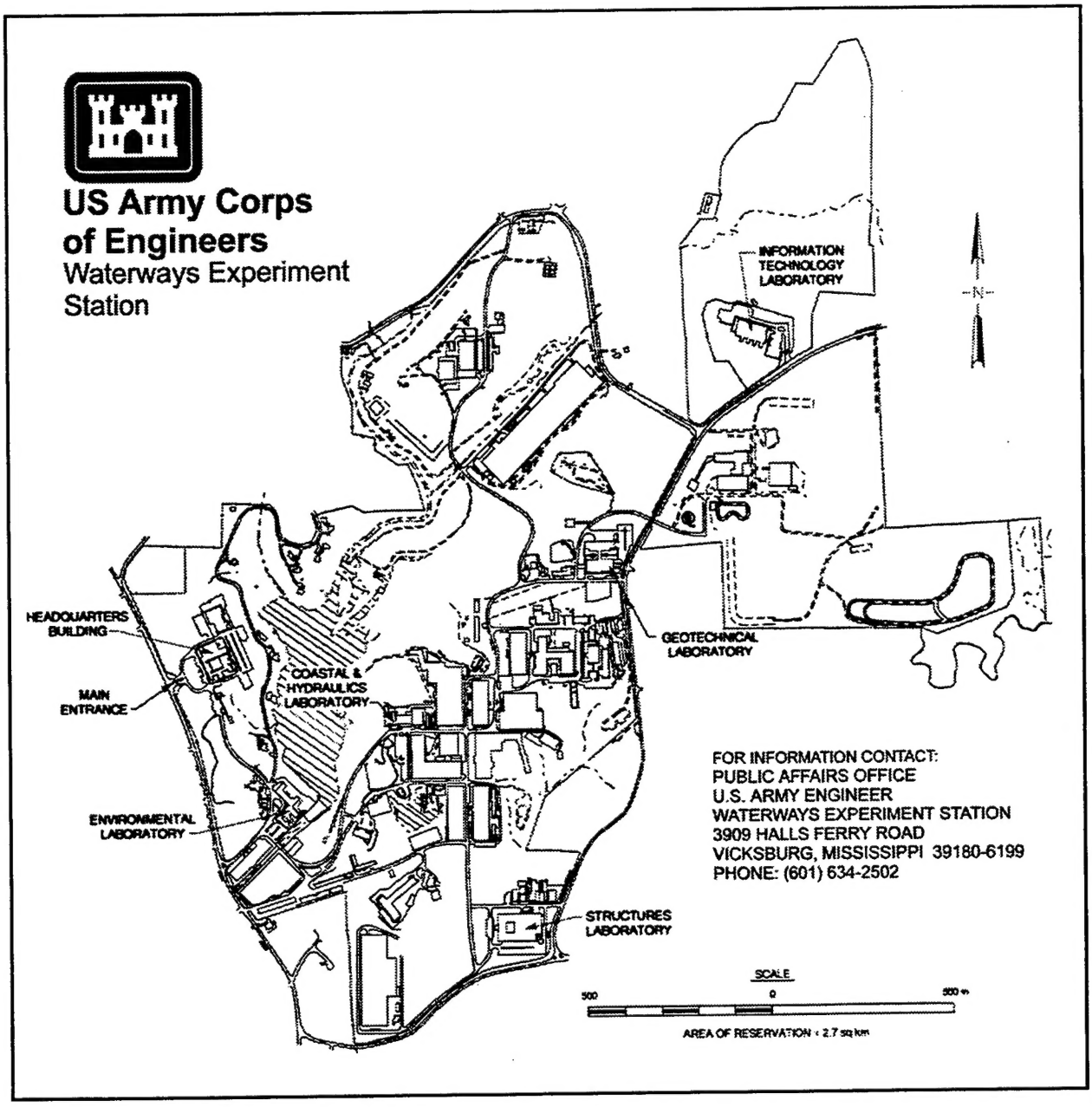

Waterways Experiment Station Cataloging-in-Publication Data

Qasim, Mohammed.
Simplified concepts in spectroscopy and photochemistry / by Mohammed Qasim ; prepared for U.S. Army Corps of Engineers.
84 p. : ill. ; 28 cm. — (Technical report ; IRRP-97-3)
Includes bibliographic references.
1. Photochemistry. 2. Spectrophotometry. I. United States. Army. Corps of Engineers. II. U.S. Army Engineer Waterways Experiment Station. III. Installation Restoration Research Program. IV. Series: Technical report (U.S. Army Engineer Waterways Experiment Station) ; IRRP-97-3.
TA7 W34 no.IRRP-97-3

Contents

List of Figures

List of Tables

Preface

The work reported herein was conducted by the Environmental Laboratory (EL), U.S. Army Engineer Waterways Experiment Station (WES), for Headquarters, U.S. Army Corps of Engineers (HQUSACE). Funding was provided by the HQUSACE Installation Restoration Research Program.
Dr. Clem Meyer was the Installation Restoration Research Program (IRRP) Coordinator at the Directorate of Research and Development, HQUSACE. Technical Monitors were Messrs. George O'Rourke and David Backer. The IRRP Program Manager was Dr. M. John Cullinane, Jr.

The report was written by Dr. Mohammed Qasim, Environmental Restoration Branch (ERB). Dr. Mark Zappi initiated the project and provided support as well as technical help throughout its writing. The late Dr. Hans Jaffe, Chairman, Chemistry Department, University of Cincinnati, served as mentor during the work pertaining to *cis-trans* photoisomerization;
Dr. Mary Jane Selgrade, Chief, Immunotoxicology Branch, Environmental Protection Agency, Research Triangle Park, North Carolina, worked on structural identification of protein dye conjugations through ultraviolet and visible spectroscopy and thin layer chromatography. Mrs. Mary Qasim constructed tables, arranged final form of document, and verified technical information and linguistics. Mr. Todd Miller, WES, contributed drawings of molecular structures. Mses. Deitdre Walker and Evelyn Toro and Mr. Jimmy Boyd, WES, obtained stopped-flow spectra, and Ms. Walker verified technical information.

The work was conducted under the direct supervision of Mr. Daniel E. Averett, Chief, ERB, and under the general supervision of Mr. Norman R. Francingues, Chief, Environmental Engineering Division, and Dr. John W. Keeley, Director, EL.

At the time of publication of this report, Dr. Robert W. Whalin was Director of WES. Commander was COL Bruce K. Howard, EN.

This report should be cited as follows:

Qasim, M. (1997). "Simplified concepts in spectroscopy and photochemistry," Technical Report IRRP-97-3, U.S. Army Engineer Waterways Experiment Station, Vicksburg, MS.

1 Introductory Statement

Photochemistry effects changes in organic and inorganic compounds which otherwise might not be attainable. Spectroscopy demonstrates the photochemical interaction between matter and electromagnetic radiation and deals with all kinds of interactions of electromagnetic radiation with a molecule whether these interactions are absorption, emission, optical rotation, or light scattering (Levine 1983). These interactions generally offer valuable information about the molecule being investigated.

Since spectroscopy is the quantum mechanical manifestation of the electronic configurational changes in atoms and molecules (as it applies to primary photochemical processes), spectroscopic techniques are powerful tools for determining both structural and quantitative changes in organic and inorganic compounds.

The reason spectroscopic techniques can ascertain the structure of compounds is because different structures absorb energies at specific frequencies or wavelengths. In other words, absorbed energy is quantized by having discrete energy levels and is specific to the particular structure. The intensity (a measure of molar absorptivity of absorbed light) is proportional to the amplitude of the wave and is also specific to the wavelength at which absorption takes place, further, this intensity is a measure for determining whether the electronic, vibrational, or rotational transition is allowed. These concepts and techniques will be discussed in this paper, with the purpose of providing useful, practical information about photochemical and spectroscopic tools that can be used by researchers. Principles of quantum mechanics will be very briefly presented; in general, the information presented in this paper is an abridged compilation from many sources and is by no means complete.

There are two basic components of this paper. The first portion consists of basic concepts needed for minimal understanding of the field; the second is comprised of a few ultraviolet (UV) and visible (VIS) applications to organic molecules, showing representative uses and examples.

Background and Basic Concepts

To understand some of the concepts presented in this paper, it is necessary to provide sufficient historical background to show their development.

In 1801, Thomas Young, in his diffraction experiments, demonstrated the wave nature of light when light waves from two adjacent pinholes in a box interfered with each other. James Maxwell, in 1860, advanced the idea that light is comprised of electromagnetic radiation, an idea proven in 1887 by Heinrich Hertz, who produced electromagnetic radiation from oscillating electrons in a wire. Hertz discovered the photoelectric effect—the ejection of electrons from a molecule when impinged by light. When the frequency is above a certain minimum value, electrons are ejected from the molecule (Bromberg 1980). The unit of frequency, Hertz (cycles per second), was named after him.

Between 1885 and 1910, Balmer, Rydberg, Lyman, Baschen, Brachen, and Pfund observed different light spectra from the hydrogen atom consistent with the equation:

$$\frac{1}{\lambda} = R\left(\frac{1}{n_1^2} - \frac{1}{n_2^2}\right) \tag{1}$$

where

n_1 and n_2 = integers

$$n_2 \leq 2$$

R is the experimentally measured Rydberg constant, which is equal to 109,678 cm^{-1}.

Niels Bohr, in 1913, postulated that the angular momentum of the orbit electron of the heated hyrdrogen atom is quantized and can have only values which are integer multiples of $h/2\pi$. Bohr found that the derived Rydberg's constant, R, is equal to $2\pi^2 me^4/h^3c$, which is the same as the experimental value (m and e are the mass and charge of the electron, respectively; c is the speed of light, and h is Planck's constant). The above equation confirms that the energy between the states is equal to

$$E_2 - E_1 = h\nu \tag{2}$$

Although it was found that Bohr's theory applied only to the hydrogen atom and could not be applied to a many-electron system, it paved the way for quantum mechanics introduced simultaneously by Heisenberg and Schrodinger.

Planck's Constant

At the turn of the century it became obvious that classical mechanical theories could not explain the spectral distribution emanating from a heated cavity (black-body radiation) or the many experimental facts pertaining to atom-size moving particles.

When a cavity of fixed size is heated to a certain temperature, the radiant energy increases and reaches a maximum only at one definite frequency. When heated to a higher temperature, the value of the maximum radiant energy increases with a slight shift toward higher frequency.

In 1900, Planck derived an accurate equation for the curves of the rate of radiant energy, M, emanating from a heated cavity of fixed size against frequency, v, where v is the frequency of waves or cycles per second. Planck proposed that electromagnetic radiation is emitted or absorbed by "oscillating dipoles." Each oscillator cannot absorb or emit an energy value or quantity different from a proton, hv (Alberty 1983). Planck calculated h by applying the experimental value of the cavity spectra to the radiant energy-frequency equation. The present value of Planck's constant, h, is 6.626176×10^{-34} Joules.seconds (or Js). Planck explained that line spectra produced from hot gases can be interpreted only as a difference between two energies

$$E_2 - E_1 = hv \tag{3}$$

Planck called this discrete unit of energy, hv (which corresponds to the frequency, v), a quantum. Quanta can be only whole number multiples of hv. This equation is one of the most important equations in spectroscopy because it forms the basis for much later development in the field.

Useful forms of the above equation are

$$\Delta E = hv \tag{4}$$

$$\Delta E = \frac{hc}{\lambda} \tag{5}$$

$$\Delta E = hc\bar{v} \tag{6}$$

where

$c = 2.998 \times 10^8$ m per sec

λ = wavelength in meters, m

The speed of light, c, is the frequency, ν, times the wavelength, λ, and the wave number, $\bar{\nu}$, = reciprocal of λ.

$$\bar{\nu} = \frac{1}{\lambda} \tag{7}$$

A useful relationship between temperature, T, and the wavelength, λ, at which the maximum radiant energy takes place, can easily be derived as the Wien displacement law,

$$\lambda_{max} T = 2.898 \times 10^{-3} mK \text{ (Alberty 1983; Atkins 1990)} \tag{8}$$

Another easily derived equation,

$$M = \sigma T^4 \tag{9}$$

relates the total radiant energy per unit time per unit area, M, emitted from a cavity with fixed size to temperature, T, where σ is the Stefan-Boltzmann constant,

$$\sigma = \frac{2\pi^5 k^4}{15h^3c^2} = 5.6697 \times 10^{-8} Js^{-1}m^{-2}K^{-4} \text{ (Alberty 1983; Atkins 1990)} \tag{10}$$

Photoelectric Effect

Einstein added to Planck's concept of electromagnetic radiation that each bundle of light, in addition to being a wave, is also particle-like and has a unit, $h\nu$, which he called a photon. Einstein's equation for the photoelectric effect can be written

$$h\nu = \frac{1}{2}m\nu^2 + V \tag{11}$$

where

V = minimum energy needed for the electron to escape a metal surface

$1/2\ m\nu^2$ = kinetic energy the electron possesses after it escapes the surface

The value of the energy, V, differs from one metal to another. Light absorption by a molecule is independent of number of quanta impinging on the molecule per second (intensity) but does depend on the minimum threshold energy possessed by each quantum. An increase in the number of photons impinging on a metal surface increases the rate of emission (intensity), whereas an increase in the frequency of light increases the kinetic energy of the emitted electron. In other words, when the frequency or energy is above a minimum threshold, the energy of light will be transferred completely to the absorbing electrons. According to Einstein, the absorption of a photon is localized; the primary, or first, absorption is where one electron completely absorbs one photon or quantum, $h\nu$, which can cause the ejection of electrons.

Compton Effect

The Compton effect is when a monochromatic X-ray impinges on a graphite target and an X-ray photon collides with an individual electron, causing the appearance of an additional light component of somewhat longer wavelength (less energy). Some energy is lost through collision, and the appearance of the light component of longer wavelength (light scattering) is caused by this energy loss.

In summary, to account for the interaction of light with matter, the dual nature of light as waves and as particles must be recognized. To explain light propagation and its reflection, refraction, and interference, light must be treated as a succession of waves or electrical and magnetic oscillations perpendicular to each other and to the direction of wave propagation. However, to understand its Compton effect or its photoelectric effect, light must be treated as bundles of particles with specific and discrete energies.

de Broglie Wavelength

In 1924, de Broglie derived his equation,

$$\lambda = \frac{h}{mv} \tag{12}$$

by relating the wavelength, λ, to is momentum, mv, where m and v are the mass and the velocity of the particle, respectively. To do this, de Broglie combined Einstein's equation $E = mc^2$ with the energy quantization equation, $E = h\nu$, substituting c/λ for the frequency, ν, where c = speed of light; in addition, he used v, the speed of the particle, instead of c, the speed of light. By this equation,

$$\lambda = \frac{h}{mv} \tag{12bis}$$

de Broglie hypothesized that the behavior of electromagnetic radiation applies also to matter; this same equation applies both to particles and to electromagnetic radiation. Later this was shown to be true experimentally. The significance of this equation is that it paved the way to quantum mechanics.

Furthermore, the de Broglie wave equation, by explaining the particle-wave dual behavior of an electron around the atom, confirms, in essence, the Heisenberg uncertainty principle that it is impossible to simultaneously determine the electron's position and momentum with precision.

Heisenberg Uncertainty Principle

The uncertainty principle states that the product of the uncertainties in both momentum and position of a particle is $\geq \hbar/2$ or

$$\Delta p \Delta x \geq \frac{\hbar}{2} \tag{13}$$

where

Δp = change in momentum

Δx = change in position (displacement of particle)

h = Planck's constant

$\hbar = h/2\pi$

The energy derived from the above equation, upon rearranging, squaring, and dividing by 2 m, becomes

$$E = \frac{h^2}{8ma^2} \tag{14}$$

where

m = mass of the particle

$a = \Delta x$

$$E = \frac{n^2h^2}{8ma^2} \tag{15}$$

The minimum energy, obtained from the solution of the Schrodinger wave mechanics equation for a particle in a one-dimensional (1-D) box becomes identical to the energy, $E = h^2/8ma^2$ (uncertainty principle) when the quantum number $n = 1$. This contrasts with classical mechanics energy equations where there are no restrictions on the value of n. Also the minimum energy (from the uncertainty principle) is identical to the energy obtained from the de Broglie equation. In addition, the de Broglie wavelength is identical to the wavelength obtained from the solution of the wave function of the Schrodinger equation.

The uncertainty principle also applies to the product of the uncertainties in time and energy

$$\Delta E.\Delta t \geq \frac{\hbar}{2} \tag{16}$$

This equation is really the same as the first equation for the product of the uncertainties in momentum and position. The product, $\Delta E.\Delta t$, it is important in determining the lifetime, τ, which is the average span of time particle stays in an excited state before reverting to the ground state. Substituting Planck's quantitized energy,

$$\Delta E = h\Delta v \tag{17}$$

which is $\Delta E = 2\pi \hbar = h/2\pi\Delta v$ into the uncertainty principle equation,

$$\Delta E.\tau \geq \frac{\hbar}{2} \tag{18}$$

yields

$$2\pi\hbar\Delta v.\tau \geq \frac{\hbar}{2} \tag{19}$$

or

$$\tau \geq (4\pi\Delta v)^{-1} \tag{20}$$

This establishes an inverse relationship between the lifetime of an excited state and its spectral bandwidth expressed in terms of frequency.

Schrodinger Equation

In 1929, at the time Heisenberg was developing his matrix mechanics, Schrodinger was postulating his wave mechanics equation. It is noteworthy that although the two methods proved to be mathematically identical, the Schrodinger wave equation, which marked a complete break from classical wave mechanics, was never derived but was judged by its correct results and predictions—which agree with experimental values obtained through spectroscopic techniques.

The Schrodinger equation can be written in its simplest form as

$$H\psi = E\psi \tag{21}$$

where

H = quantum mechanical Hamiltonian operator, which contains both kinetic and potential energy components

E = total energy

ψ = time independent wave function, which completely describes the state of the system at a specific time

The significance of ψ is when used with its conjugate, ψ^*, over the differential volume element, $d\tau$, at a specific time, t, the product, $\psi^*\psi d\tau$, is real and represents the probability for finding the particle within the volume element, $d\tau$.

A simplification of the wave equation considers the motion of a particle within a 1-D box in the x direction in which the Schrodinger equation becomes

$$H\psi_x = E\psi_x \tag{22}$$

and the probability density along the x axis can be $\psi_x^* \psi_x$ or $|\psi^2|_x$. The probability density is real and finite; the wave function, ψ, is well-behaved and a single-valued.

The classical Hamiltonian operator is

$$H = \frac{1}{2m} p^{2_x} + V_x \tag{23}$$

where

p = momentum, mv

V_x = potential energy

In quantum mechanics p_x is replaced by

where

$$i = \sqrt{-1}$$

$$\hbar = \frac{h}{2\pi}$$

The I-D Schrodinger equation becomes

$$\frac{-\hbar^2 d^2 \psi_x}{2mdx^2} + V_x\psi = E\psi_x \tag{24}$$

To avoid discontinuity, ψ must = 0 at x = 0 and at x = a. Within the free space of the 1-D box whose length is a, $V_x = 0$. Thus the wave equation reduces to

$$-\frac{\hbar^2 d^2 \psi_x}{2mdx^2} = E\psi_x \tag{25}$$

There are two satisfactory solutions to this equation for the allowed energies:

$$\psi_1 = Ae^{ikx} \tag{26}$$

or

$$\psi_1 = A^1 \sin kx \tag{27}$$

$$\psi_2 = Be^{-ikx} \tag{28}$$

or

$$\psi_2 = B^1 \cos kx \tag{29}$$

where

A, A^1, B *and* B^1 = arbitrary constants and $k = \frac{1}{\hbar}\sqrt{2mE}$

The above solutions represent traveling waves, where $\lambda = \frac{2\pi}{k}$

Therefore, substituting for k gives

$$\lambda = \frac{h}{mv} \tag{30}$$

This wavelength, λ, obtained as a solution of the Schrodinger equation, is identical to the de Broglie wavelength.

It can also be shown that within the box,

$$\frac{2\pi}{h}\sqrt{2mE}\, a = n\pi \tag{31}$$

which gives

$$E = \frac{n^2h^2}{8ma^2} \tag{32}$$

where

a = length of the free path of the particle in the 1-D box

n = integer quantum number with a minimum value of 1

This energy equation is the same as that obtained from the de Broglie or the Heisenberg uncertainty principle and contrasts with the energy equation obtained from classical mechanics where n can be of any value.

2 Basic Tools

Needed basic tools will be briefly discussed in this chapter, namely: Lambert-Beer Law (the thoretical basis for absorbance-concentration measurements); the spectrophotometer (first, different spectrophotometers for different regions of the spectra, and second, basic differences between emission and absorption spectrophotometers); the monochromator (the component of a spectrophotometer where wavelength separation takes place); and lasers.

Lambert-Beer Law

Spectroscopy is a direct application as well as the manifestation of quantum mechanical concepts. The Lambert-Beer Law constitutes the basis of spectroscopic analytical methods and can be used for concentration measurements in the UV, VIS, and infared (IR) regions. Therefore, the Lambert-Beer is discussed here and can be written as

$$A = \log \frac{I_0}{I} = \in cl \tag{33}$$

where

A = absorbance

I_0 = intensity light, quanta s^{-1} per unit area

I = intensity of the transmitted light not absorbed by the sample

c = concentration of the sample in moles per liter

l = sample cell length in centimeters

$\in$ = (which used to be called the molar extinction coefficient) = molar absorptivity, a measure as to whether an electronic or vibrational transition of a molecule is allowed at a certain wavelength

To derive the Lambert-Beer Law, simply consider a light beam with intensity I_0 impinging on a sample of concentration, c, in a cell which is 1 cm long. I_0 decreases with small increments, dl, of the cell length (Figure 1). Then

$$\frac{dI}{dl} = -kcI \tag{34}$$

or

$$\int_{I0}^{I} \frac{dI}{I} = -kc \int_{0}^{l} dl \tag{35}$$

which becomes

$$In \frac{I_0}{I} = kcl, \text{ or using base 10 logarithm} \tag{36}$$

$$\log \frac{I_0}{I} = \in cl = \text{the absorbance, A,} \tag{37}$$

where

$\in = 2.3k$

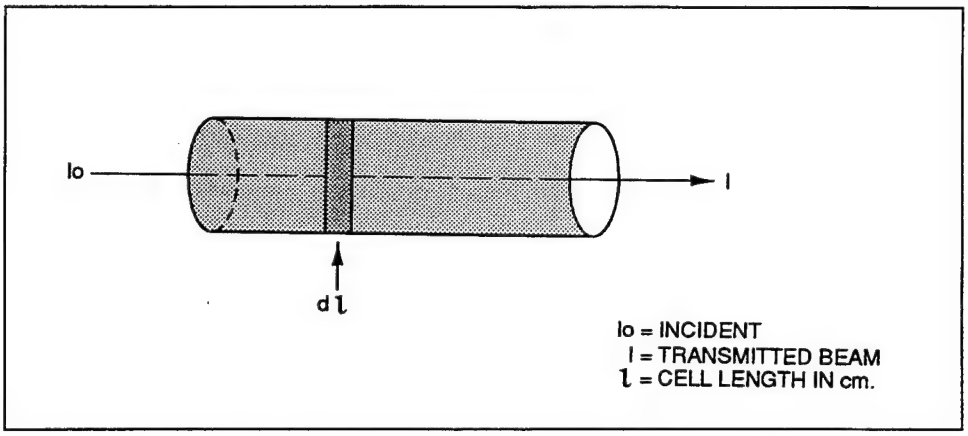

Figure 1. Sample cell

Instrumentation

Spectrophotometers measure changes in the spectra; irradiation devices effect these changes.

It is important to explain the basic components of that powerful tool, the spectrophotometer. These components of the spectrophotometer depend first on which spectral region (IR, UV, VIS) is being investigated and second according to whether absorption or emission is being studied.

Similarities and differences between the absorption spectrophotometers in the UV, VIS, and IR regions

The basic components of a spectrophotometer in the IR, VIS, and UV regions are similar; the main differences are in the sources and sample cells. The source in the IR is a metal or ceramic heating element, which emits heat or vibrational energy, whereas the source for the UV is an electron tube, such as a deuterium light, and the source used in the VIS region is a tungsten filament light bulb.

The sample cell in each one of the spectral regions must be transparent to electromagnetic radiation in that region and also inert to the sample being measured. In the IR region, the sample cell is made of salt, such as sodium chloride or potassium bromide. Although the sample cell in the VIS region can be quartz (fused silica) or glass, a sample cell in the UV region must be transparent to UV radiation and therefore is made only from fused silica.

Similarities and differences between the absorption and the emission spectrophotometer

Figures 2 and 3 represent schematic diagrams of single-beam absorption and emission spectrophotometers, respectively. The typical components of an absorption or emission spectrophotometer are: light source, monochromator, sample cell, detector, and convenient display device.

The main difference between the absorption and the emission spectrophotometer is that in the absorption spectrophotometer, the source, monochromator, sample cell, and detector are all in a line with the beam emanating from the light source, whereas in the emission spectrophotometer, a second monochromator and the emission detector are in line with a slit opening in the sample compartment perpendicular to the beam emanating from the light source. Thus, in the emission spectrophotometer, the sample becomes a secondary source of radiation; the only light reaching the detector is that emanating from the sample itself.

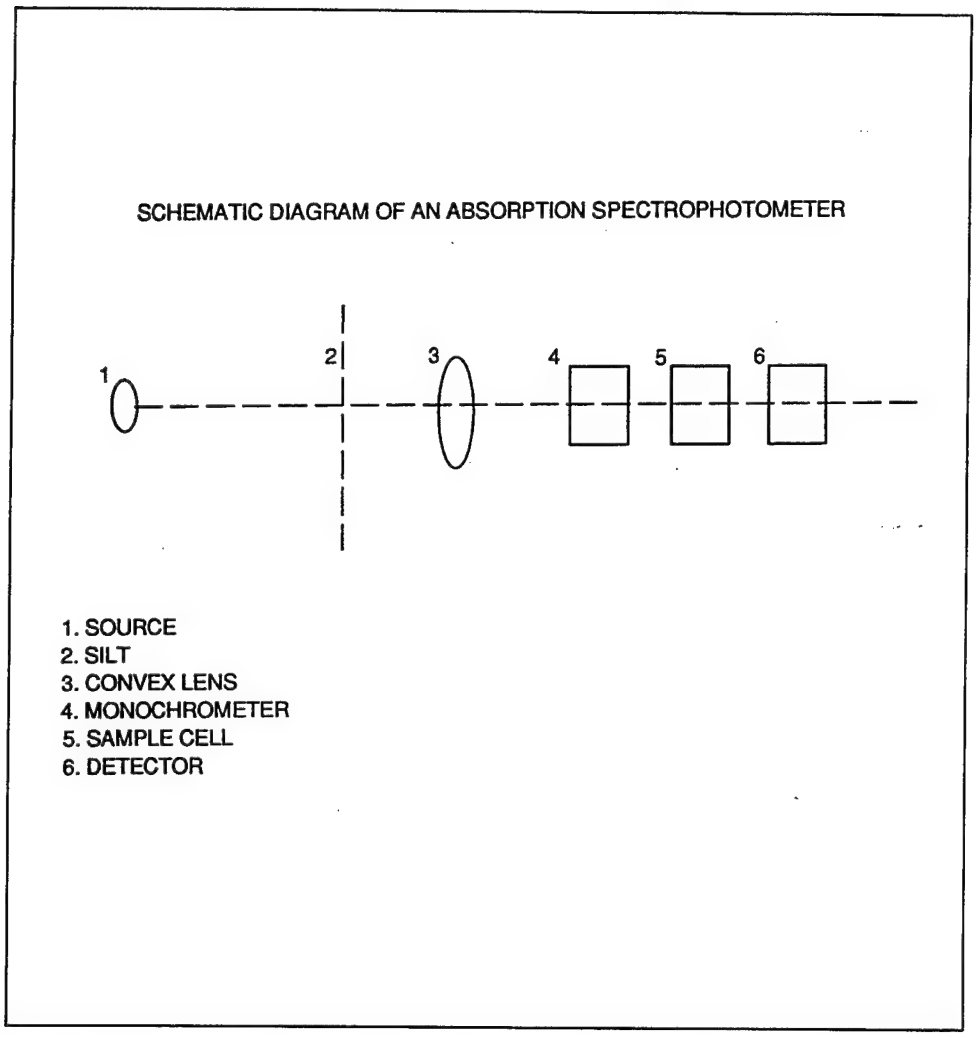

Figure 2. Schematic diagram of an absorption spectrophotometer

Grating monochromator

The gratings of these monochromators consist of a larger number of parallel lines engraved on a metallic surface. When a beam of monochromatic light falls on a grating, each line of the grating becomes a secondary source of radiation, emitting light in many directions. At certain positions on the opposite side of the grating, wavelengths in phase will accentuate each other, whereas at other positions, wavelengths not in phase will form destructive interference with each other. Thus, a pattern of bright lines with dark spaces between them will be formed. Since each wavelength has its own deflection angle, the many wavelengths of irradiation will separate upon impinging on the grating. Using Young's experiment for wavelength interference, it can be shown that the action of an incident beam of light falling perpendicularly on a grating can be described by the following equations:

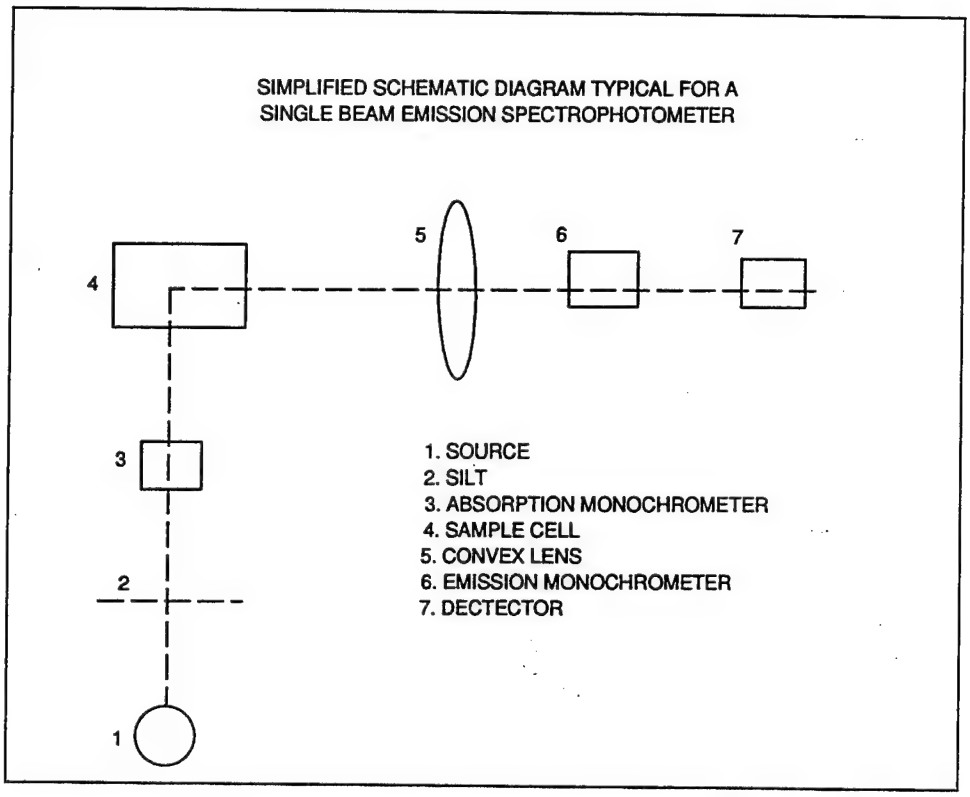

Figure 3. Simplified schematic diagram typical for single-beam emission spectrophotometer

$$n\lambda = d\sin\theta \text{ for bright lines} \qquad (n = 0,1,2,3\ldots) \tag{38}$$

$$n\lambda = 2d\sin\theta \text{ for dark spaces} \qquad (n = 1,3,5\ldots) \tag{39}$$

where

n = order of deflection

d = distance between the lines

θ = angle of deflection

λ = wavelength of incident radiation

The last of the two above equations is the same as the Bragg equation used in X-ray, crystallography, $n\lambda = 2d\sin\theta$, where n = order of diffraction and equals 0,1,2,3...; d = the spacing between particles; θ = angle of X-ray diffraction; and θ = wavelength of incident X-ray radiation.

Lasers (Light Amplification by Stimulated Emission of Radiation)

Lasers are produced by stimulated emission when more than two electronic energy levels are involved. An upper energy state, *m*, can be populated by very intense irradiation with appropriate frequency whereas an intermediate energy level, *l*, can be populated indirectly by radiationless processes from the upper level. If there is no incident irradiation on the middle or intermediate level, this level might lose its excitation and drop down to the ground state, *k*, only through spontaneous emission, which is much less efficient than stimulated emission. This would, therefore, result in an inversion of population where the intermediate state becomes more populated than the ground state (Figure 4).

The laser system is placed in a cylinder with two highly polished parallel mirrors, one at each end and one of which is partially silvered. The distance between the system and the mirrors is proportional to integer wavelengths, $n\lambda$, between the ground state, *k*, and the intermediate state (Figure 5).

Low-intensity spontaneous emission from the intermediate state multiplies as it is reflected back and forth into the mirrors along the axis of the cylinder, inducing a coherent, intense, and very monochromatic laser beam along the axis. It is important to note that in spontaneous emission, the molecule emits in random direction and phase, whereas in stimulated emission, the emission is in direction and phase of the beam.

Among the many uses of lasers:

a. Lasers, due to their monochromaticity and coherence, are selective for specific photochemical reactions.

b. Lasers can be used to study very fast reactions (picoseconds) because of their short durations (Bromberg 1980).

c. Lasers are perfect tools for detecting weak lines in Raman spectra because of their very high intensity and monochromaticity.

d. Lasers can selectively ionize or dissociate a specific isotope in a molecule and therefore can be used for the separation of isotopes (Alberty 1983).

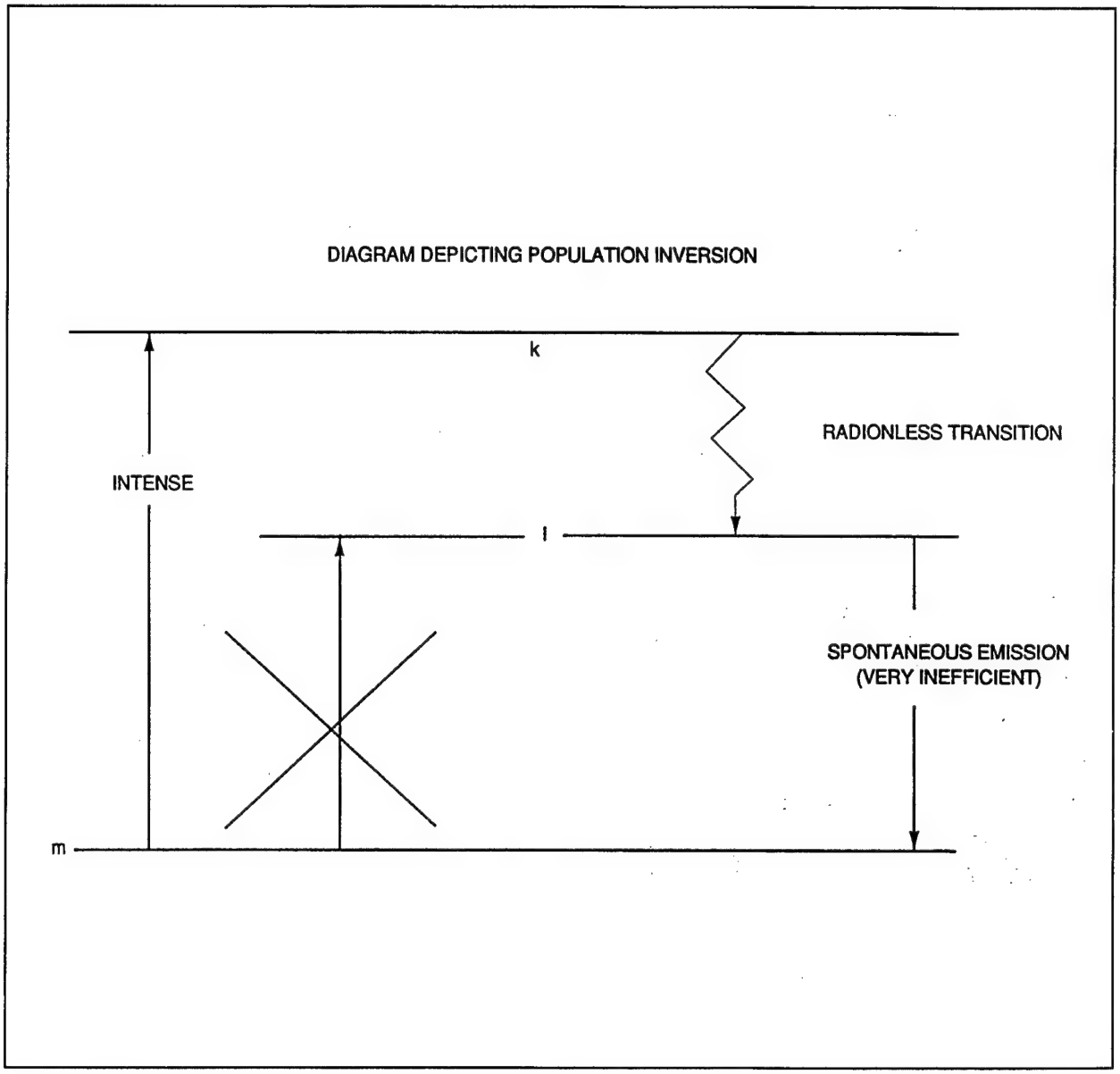

Figure 4. Diagram depicting population inversion

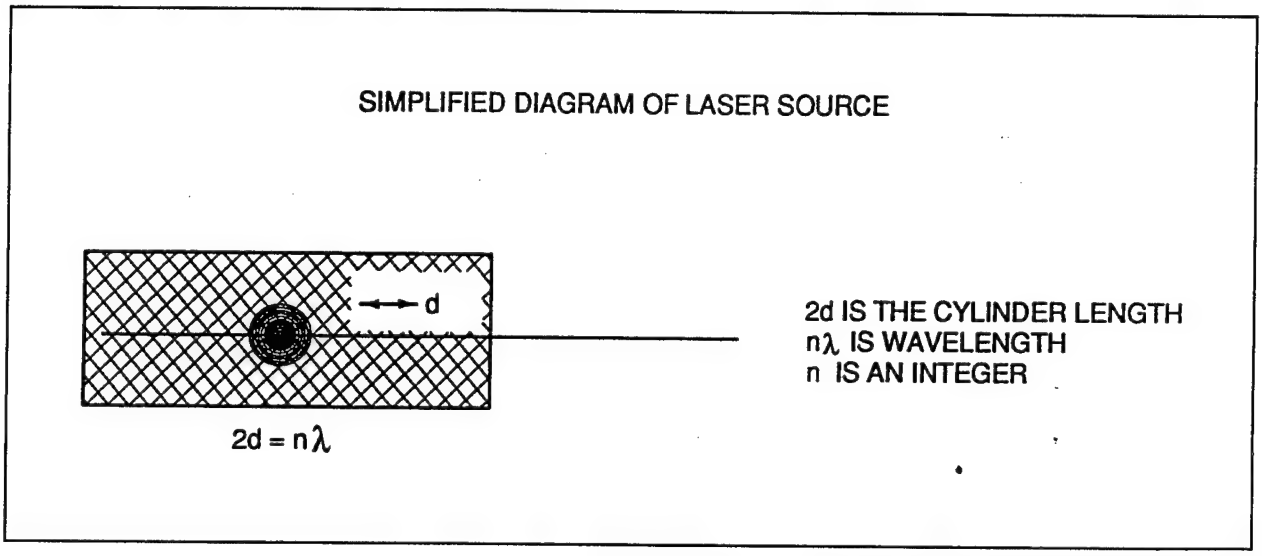

Figure 5. Simplified diagram of laser source

3 Regions of Electromagnetic Radiation

The useful spectra of electromagnetic radiation covers a wide range of energies. Each region, due to differences in energy, unfolds useful and varied information about the molecules being studied. Although these regions represent different energies, the equations pertaining to these various regions are quite similar. Table 1 summarizes the functions and indicates the magnitude of energies, frequencies, and wavelengths for the different parts of the electromagnetic spectra. These regions are briefly discussed, the main emphasis being on electronic excitations, UV, and VIS spectra. The order in dealing with most of the spectral regions is from shortest to longest wavelengths.

X-Rays

X-rays are produced when a high-energy electron beam, more than 30 Kev, strikes a target atom, typically metal atoms. X-rays produce spectra which show continuous intensity curves with superimposed sharp peaks. The continuous curve and discrete sharp peaks can easily be understood through quantum mechanics. The continuous part of a typical X-ray curve originates as the electron is slowed or stopped; part of the electron's kinetic energy is converted to electromagnetic radiation (X-rays) as it slows. However, when the electron is completely stopped by the particle, all of its kinetic energy is completely converted to X-rays (light quanta, $h\nu$) (Bromberg 1980). Increasing the energy of the striking electron manifests itself by shifting the X-ray continuous spectra toward shorter wavelengths (higher energy).

The discrete peaks are due to transitions of electrons between the inner orbits of the target atoms (unlike UV and VIS spectra, which are due to electronic transitions between the outermost orbitals). When an electron is ejected from an inner orbit, an electron from a higher orbit falls down to replace it, causing emission of X-ray radiation. X-ray crystallographers use special designations for these inner shell electronic transitions, such as K_α and K_β and as L_α and L_β, etc.

Table 1
Properties of Various Regions of Electromagnetic Radiation

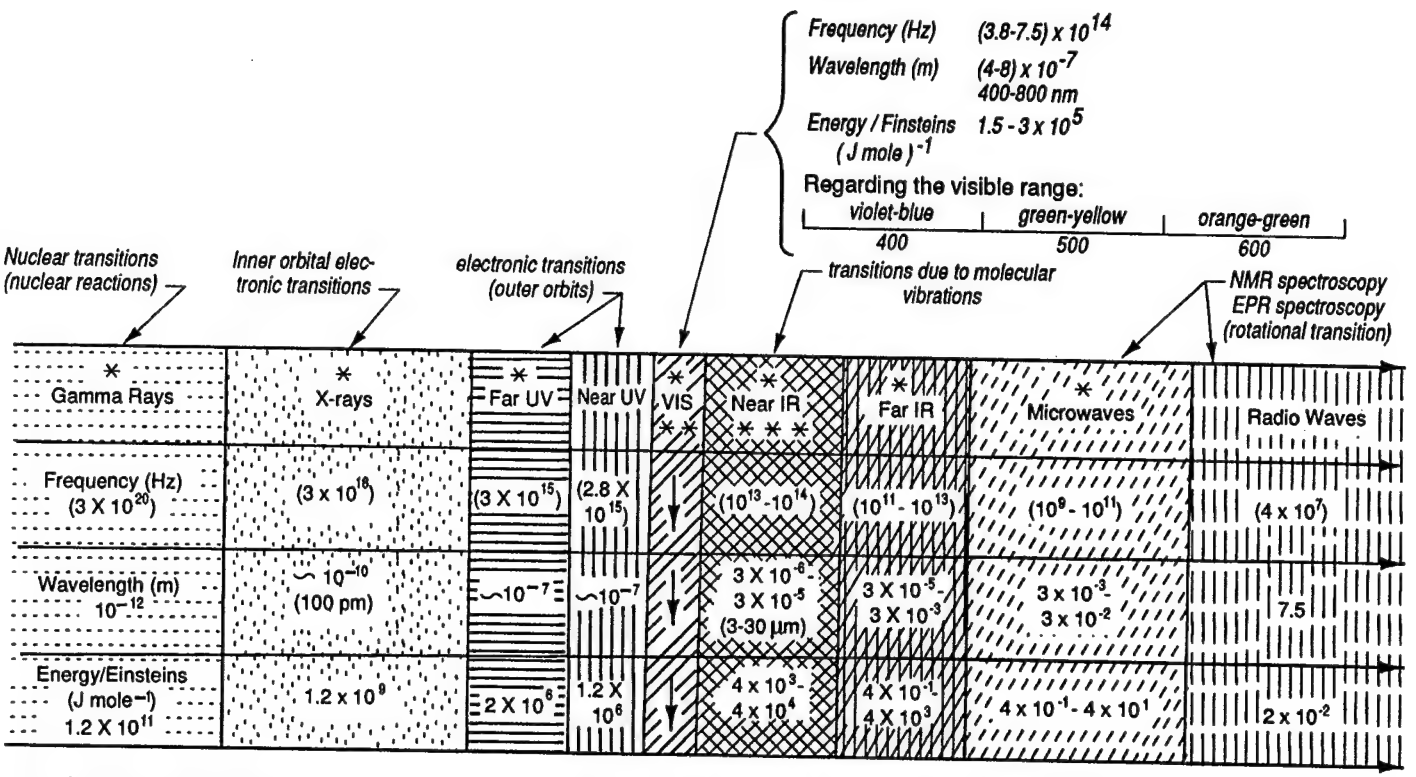

* Atomic or molecular processes associated with each region

* * Electronic transitions (outer orbits)

* * * Rotational transitions of light molecules; vibrational transitions

Note 1: The value of an Einstein, ΔE, is $1.196 \times 10^{+1}/\lambda$ (m) Joules mol^{-1}

Note 2: All values represent an approximate average range and not a particular value

Note 3: The near UV/VIS region ranges from 200 nm (6.2 eV) to 700 nm (1.8 eV).

A very important relationship, which establishes the basis for the present periodic table of the elements, was Mosely's finding (1913-1914) that the squares of the atomic numbers of the various elements are directly proportional to their $K\alpha$ X-ray frequency (Bromberg 1980).

X-rays are useful in identifying structures of organic and inorganic crystals by showing adjacent particles and determining the distances between. X-ray crystallography takes advantage of the fact that X-rays are of the same magnitude as bonds between atoms, approximately 10^{-10} m by using Bragg's equation,

$$n\lambda = 2d \sin \theta \tag{40}$$

where

n = integer

λ = wavelength

θ = angle of diffraction

d = distance between particles

UV and VIS Regions of the Spectra

The ease of electronic transition from the ground to a higher excited state dictates whether the observed wavelength is in the UV or VIS region. UV and VIS spectra offer valuable information for identifying compounds, especially by the use of their emission (See paragraph, Fluorescence and phosphorescence).

This region also gives information about the electronic behavior of compounds and about ongoing changes due to chemical reactions.

UV and VIS spectra are the most useful regions for concentration measurements through use of the Lambert-Beer law. Molar absorptivities depend on the compound, the wavelength, and the solvent and are a measure as to whether an electronic transition is allowed. The magnitude of molar absorptivity is proportional to intensity which is, in turn, proportional to the electrons undergoing transition.

Singlet and triplet electronic excited states

An electronic excited state can be represented as $2S+1$, where S is the total electronic spin quantum number. Each electron possesses + or - 1/2 spin quantum number.

In a singlet state, the electron spins cancel each other, $S = 0$ or $2S+1 = 1$, whereas in a triplet state, the total electron spin, $S = 1$ or $2S + 1 = 3$.

For example, fluorescence emanates from singlet states where $\Delta S = 0$; however, with phosphorescence, $\Delta S \neq 0$.

Fate of the electronic excited states

When a molecule absorbs a photon or quantum ($h\nu$) of UV or VIS light, an electron is promoted from the singlet ground state, S_0, to an excited singlet state in about 10^{-15} seconds. In about 10^{-11} seconds, some of the energy will be lost by internal conversion, and the electrons drop to the first excited singlet state, S_1. A typical lifetime of this first excited singlet state is between 10^{-8} and 10^{-7} seconds.

At this time, the electron might drop (due to nonradiative intersystem crossing) to the first excited triplet state. This state, T_1, generally has lower energy than that of the first excited singlet state, S_1, but higher than the ground singlet state, S_0. The electron in the first excited triplet state might lose its energy and drop to the singlet ground state by the radiative process, fluorescence, or by nonradiative processes. Or, if the first excited triplet state is close enough to the first excited singlet state, the electron might gain sufficient vibrational energy to cross over to the first excited singlet state and then lose its excess energy by delayed fluorescence to the ground singlet state.

When the electron is in the first excited singlet state, energy might also be lost by the radiative process of fluorescence. Eventually the electron will lose its excess energy due to: chemical reactions (isomerization, oxidation, decomposition, etc.); emission (fluorescence and phosphorescence); or heat. Thus several competing processes exist at the same time. (Figure 6).

Fluorescence and phosphorescence

Fluorescence and phosphorescence are two very important phenomena that deserve special attention. Fluorescence is the radiative emission of light from an electronic excited singlet state to the ground state, whereas phosphorescence involves emission from the lowest excited triplet state (which is lower than the first singlet state) to the ground state, which causes phosphorescence to appear at longer wavelengths. A fluorescence spectrum of a compound appears to be a mirror image of its absorption spectrum and does not involve a geometric change of the molecule. A phosphorescence spectrum, on the other hand, does not appear as a mirror image of the absorption spectrum of the compound and might be accompanied by a geometric change in the molecule.

Figure 7 illustrates the absorption and emission spectra of *trans* 2-(p-dimethylaminobenzylidene)-4-butyrolactone and shows mirror imaging and

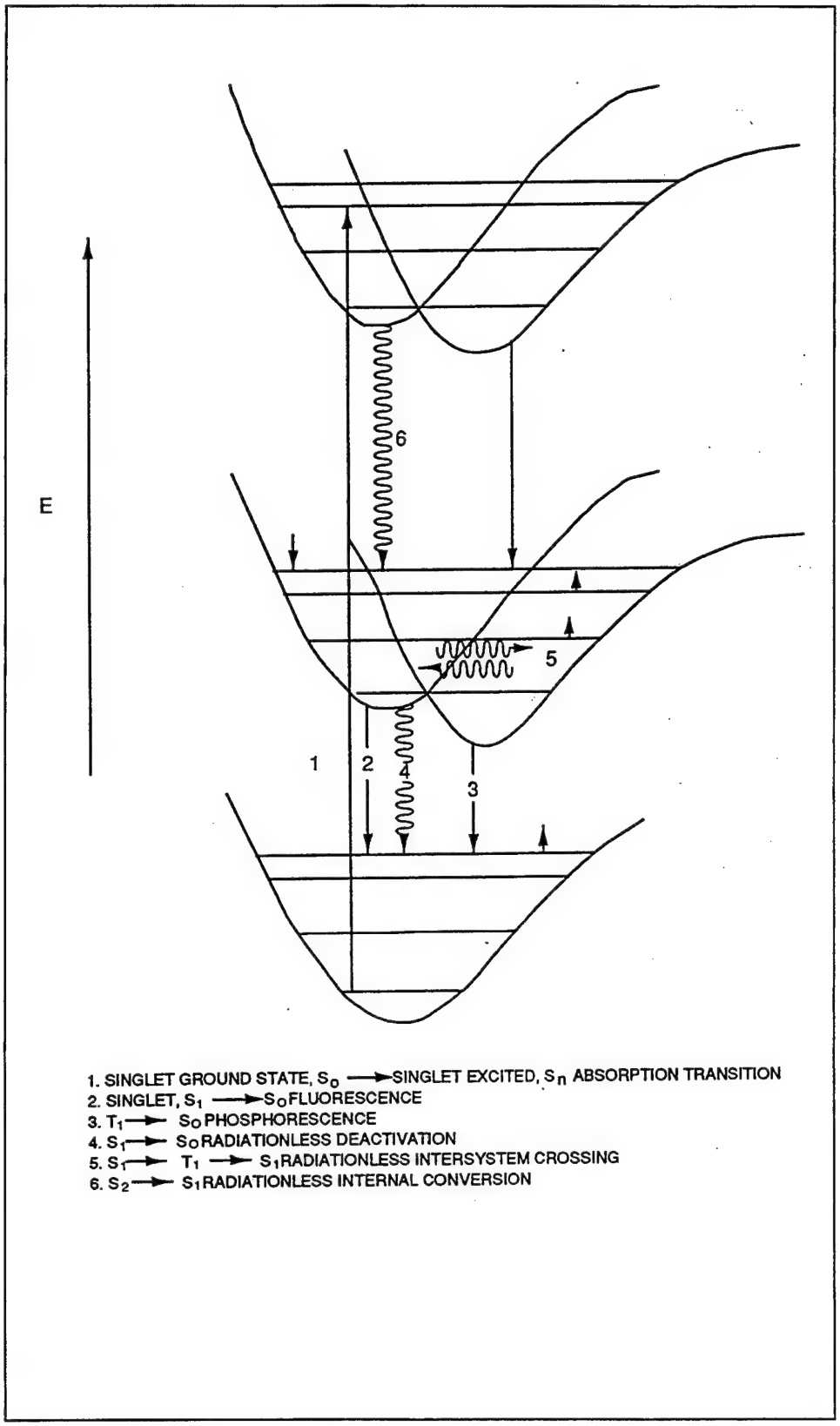

Figure 6. Simplified energy diagram showing the fate of the electronic excited states

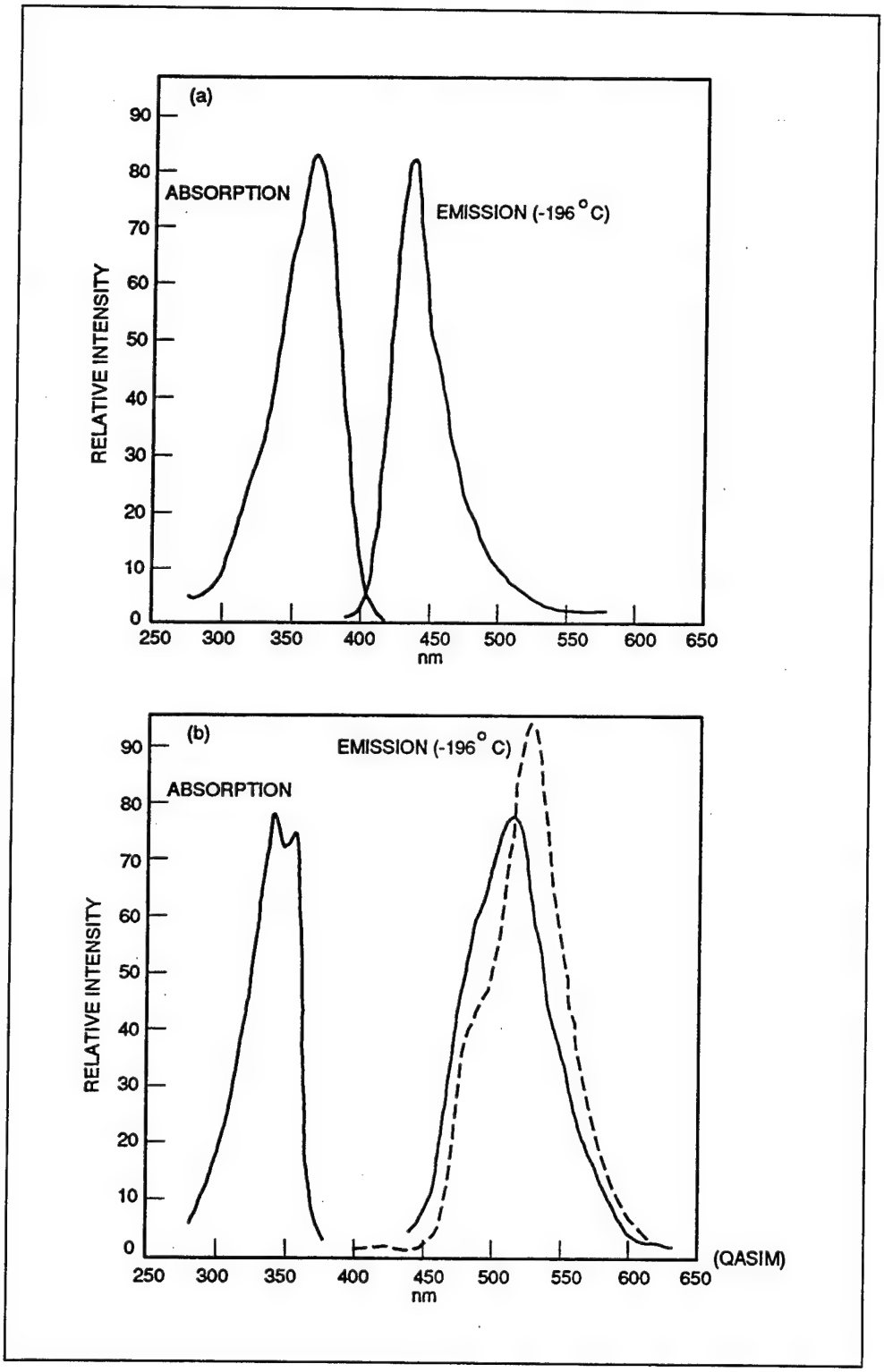

Figure 7. Absorption and emission spectra of *trans* 2-(p-dimethylaminobenzylidene)-4-butyrolactone

delayed fluorescence and phosphorescence. A detailed study of the photoisomerization of this molecule has been made, and therefore it will be used as a model; discussion of its absorption and emission spectra is in Chapter 5 regarding some applications of UV and VIS spectroscopy to organic molecules. A significant finding is that a *trans* isomer sample dissolved in MCIP in a sealed glass tube exhibited totally reversible green phosphorescence at 196 °C and delayed blue fluorescence at 78 °C, demonstrating a clear example of thermal intersystem crossing between the first excited singlet and triplet states.

Figure 8a shows a structural representation of the photochemical interconversion of *cis-trans* 2-(p-dimethylaminobenzylidene)-4-butyrolactone.

Fluorescence is an "allowed" while phosphorescence is a "forbidden" electronic transition, which accounts for the facts that fluorescence is intense and instantaneous (10^{-8} sec) and that phosphorescence is less intense and much slower (10^{-2} - 10^{2} sec). Therefore, other quenching processes might be able to compete with phosphorescence except at low temperatures where rates of quenching are much reduced.

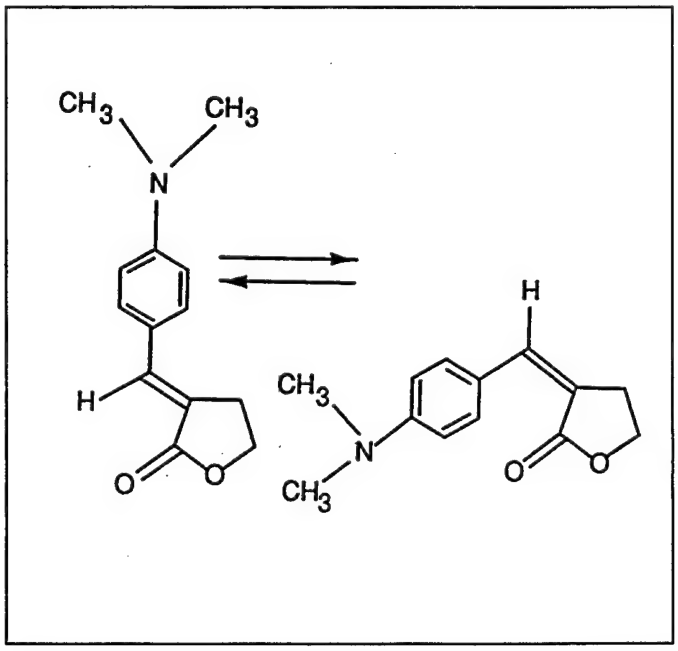

Figure 8a. Structural representation of *cis-trans* photochemical interconversion

Emission radiation from a molecule usually takes place at a wavelength between 30 and 50 nm longer than that of the exciting wavelength. This difference, known as the Stokes shift, is due to loss of energy in the excited state caused by vibrational relaxation (Gillespie 1985).

Other spectroscopic concepts that must be considered because they sometimes constitute interference with fluorescence and phosphorescence are the light scattering mechanisms that arise for various reasons, such as the Rayleigh scatter. This light scatter is due to the interface interaction between the exciting photons and the air cell, the cell wall solution, and the material suspended in the solution, making it more difficult to separate the excitation from the emission spectra (Gillespie 1985).

Raman scattering (discussed later in more detail) appears at longer wavelengths than that of the exciting light. This phenomenon is due to the

interaction of the bonds of the solvent molecules with the photons of the exciting light.

Emission spectra (fluorescence and phosphorescence) are more sensitive than absorption spectra for qualitative and quantitative measurements because of their higher intensity.

Triplet sensitizers

Absorption of light energy by a compound used as a triplet sensitizer populates the corresponding triplet state of the compound to be measured. This in turn results in p-type delayed fluorescence. A good triplet sensitizer is one with a higher triplet, but lower singlet, state than those of the compound to be sensitized. A good sensitizer also absorbs at a different wavelength than the other components in the solution. Using the triplet sensitizer technique, compounds with concentrations as low as 10^{-9} M could be detected. (Parker 1966).

Quantum yield

This useful concept can be defined in several operative ways. For instance, quantum yields can be evaluated for either absorption or luminescence (fluorescence and phosphorescence). For absorption, quantum yield is the fraction of a molecule that can absorb a quantum of radiation energy, i.e., the number of molecules per quantum of energy—or the number of moles per Einstein of energy absorbed. For fluorescence, quantum yield is defined as the ratio of the number of molecules emitting radiation to the total number of molecules excited (Gillespie 1985) or, simply, quantum yield can be looked at as a ratio of photons emitted to those excited. Fluorescence quantum yield is directly related to the mean lifetime of the excited singlet state, fluorescence intensity, fluorescence rate constant, intersystem crossing, and to the rate constant for internal conversion.

Quantum yield calculations also shed light on nonradiative processes and therefore on the fate of excited states and their mechanisms. In addition, large quantum yields are indicative of free radical involvement since these produce chain reactions.

Quantum yield measurements were used to shed light on the photochemistry involved in the *cis-trans* interconversion. Since quantum yield reflects the ratio of the rate of photochemical isomerization to the rate of light absorption, a knowledge of the number of quanta absorbed per unit time is necessary. The fraction of light absorbed by either isomer can be determined only if the light flux incident on the system is known. This is turn was determined by chemical actinometry.

Since the values of the quantum yield measurements (between 400 and 300 nm) of the *cis-trans* photochemical isomerization of the sample compound, 2-(p-dimethylaminobenzulidene)-4-butyrolactone, have been accurately determined, and since quantum yield values (plus nuclear magnetic resonance (NMR) measurements) indicate no significant competing mechanisms with the photochemical isomerization, this makes the compound a perfect chemical actinometer (Figure 8b).

Quantum yields for the photochemical interconversion were determined at room temperature over a wide range of excitation wavelengths in the most intense absorption band and in both absolute alcohol (polar) and in heptane (nonpolar). The relative quantum yields for the two isomers in both solvent systems at the various wavelengths of irradiation are listed in Table 2 and the absolute quantum yields are shown in Table 3. These quantum yields are derived from the ratios of the photostationary state concentrations of the two isomers multiplied by their respective molar absorptivities.

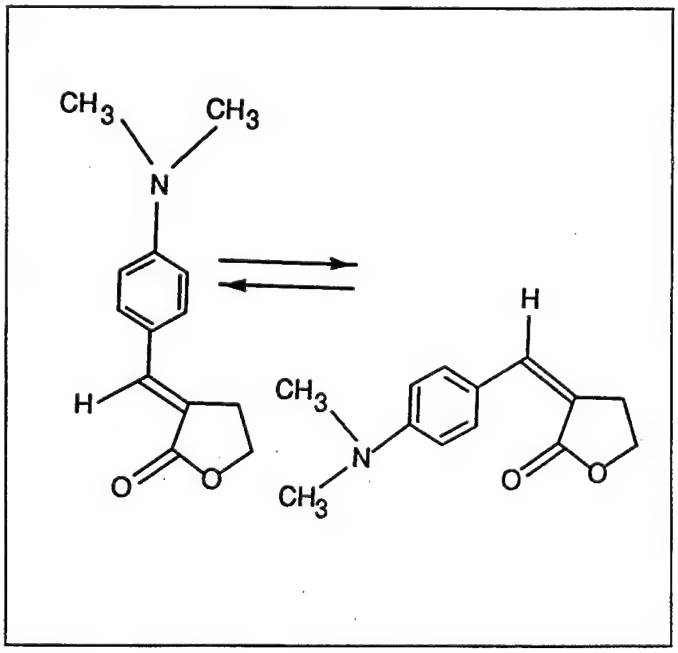

Figure 8b. Structural representation of *cis-trans* photochemical interconversion

Quantum efficiency of the *cis* is less than that of the *trans* isomer in both solvent systems, especially in heptane. Also, the quantum efficiency of both isomers, particularly that of the *trans* isomer, is lower in alcohol than in heptane. The quantum yields of the *cis-trans* isomers in both solvent systems were quite high; however, their sum was less than unity (although in heptane it was close to one). The quantum yields appeared to be independent of the irradiation wavelengths for most of the range. In addition, thermal conversion from the *cis* isomer to the *trans* isomer showed that the singlet ground state of the *trans* is lower in energy than that of the *cis* isomer.

Although complete elucidation of the photochemistry involved in the *cis-trans* interconversion has not been accomplished, some important information regarding the mechanism was obtained and is discussed under the fate of electronic excited states. Figure 9 represents a schematic diagram of a monochromatic irradiation system that affects photochemical changes while measuring the number of quanta corresponding to these changes.

Table 2
Relative Quantum Yields for *cis-trans* Photoisomerization

$$\frac{\phi c \ \infty \ \epsilon t \ x \ \% t \ at \ photostationary \ state}{\phi t \ \infty \ \epsilon c \ x \ \% c \ at \ photostationary \ state}$$

Heptane System			Alcohol System	
Wavelength, *y*, nm	Experimental direction		Experimental direction	
	t- c	c- t	t- c	c- t
400			0.77	0.86
390			0.74	0.89
380			0.81	0.88
370	0.50[1]	0.60[1]	0.78	0.79
360	0.70	0.80	0.77	0.77
350	0.70	0.81	0.78	0.75
340	0.70	0.81	0.78	0.75
340	0.70	0.75	0.81	0.71
330	0.74	0.68	0.93[2]	0.61

[1] Not reliable due to the very small molar absorptivity of the *trans* isomer at this wavelength.
[2] Not reliable because conversion to the photostationary state was not completely attained, due to weak light intensity at this wavelength.

Table 3
Absolute Quantum Yields for *cis-trans* Photoisomerization 2-(p-dimethylaminobenzulidene)-4-butyrolactone in Heptane and Alcohol

	Heptane System		Alcohol System	
y, nm	ϕt	ϕc	ϕt	ϕc
400			(0.49)	0.42
390			(0.37)	0.33
380		0.42[1] 0.45	0.37	0.31
370	(0.65)	0.39	0.34	0.27
360	(0.48)	0.38	0.34	0.27
350	(0.49)	0.40	0.39	0.34
340	0.50	0.39	0.42	0.37
330	0.47	0.41	0.57	0.53

Note: The least reliable quantum yield measurements were at the wavelengths presented at the beginning and end of the table, and were due to the low absorptivities of the isomers an to the low intensity of the light sourse.
ϕt values between brackets were calculated from experimental ϕc and their relative quantum yields, where error in obtaining experimental ϕt has been amde. Good correlation coefficients and standard deviation of the corresponding ϕc values indicate that these calculated ϕt values are quite accurate.
[1] Calculated on the basis of no photchemical reversal from *trans* to *cis* at 380 nm.

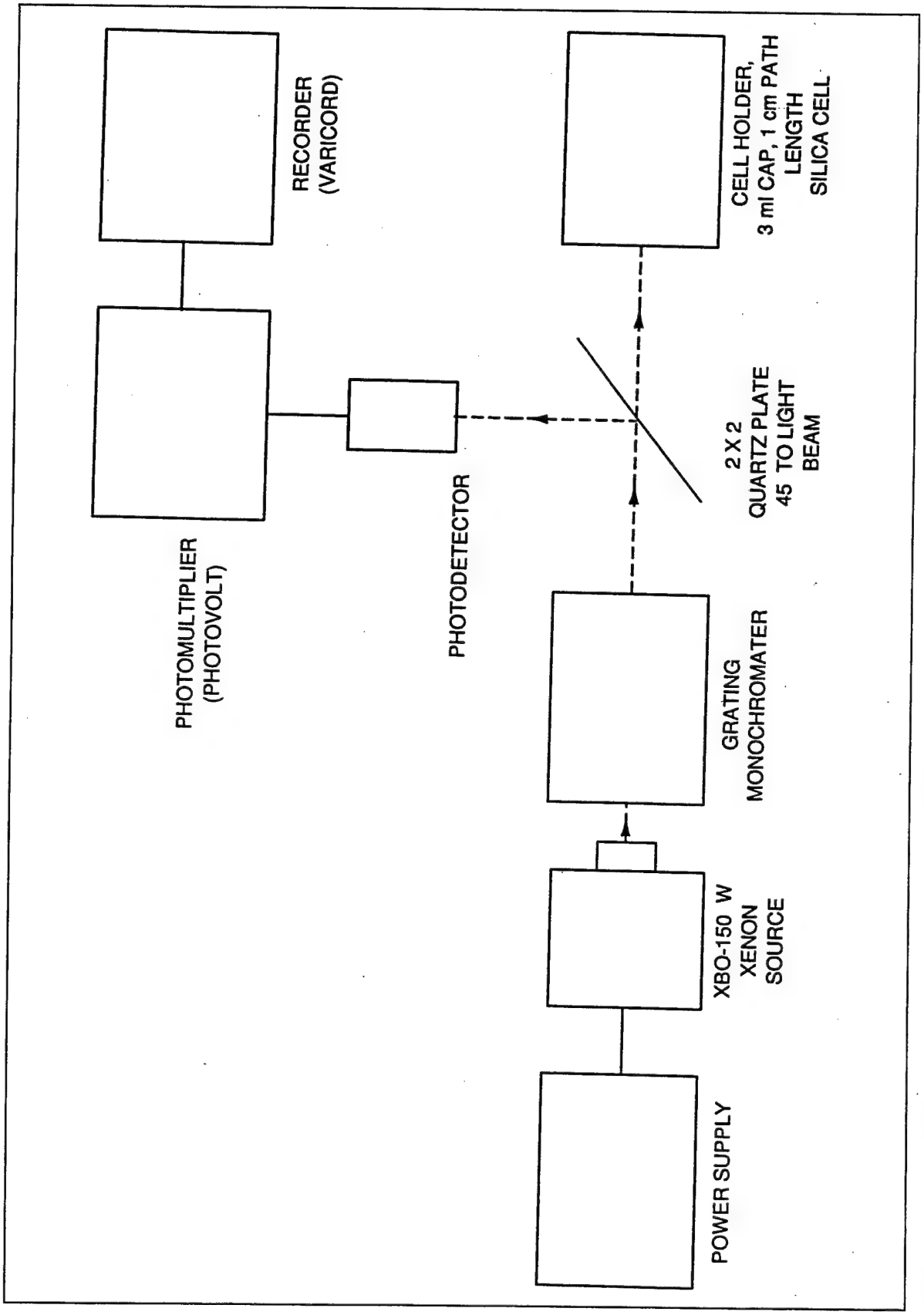

Figure 9. Schematic diagram of monochromatic irradiation system

Pi and sigma electrons

Electronic excitations or transitions in organic molecules may involve n, sigma or pi electrons:

n electrons are the nonbonding or unshared electrons such as the four sp^3 electrons on the oxygen molecule in water or the two nonbonding sp^3 electrons on the nitrogen in ammonia.

π electrons are the electrons in the pi orbitals which overlap (if they are bonding) side to side in double and triple bonds above and below the axis between two atoms.

σ electrons are the electrons in the sigma orbitals which overlap (if they are bonding) head to head along the axis between the two bonded atoms. The sigma electronic density has circular symmetry along the axis of the bond. All single bonds are sigma bonds.

Examples of the last two types of electron bonding, for instance, are the double bond between the two carbons in ethylene, which has one sigma and one pi bond, and the triple bond in acetylene, which has one sigma and two pi bonds.

The following are some observations involving n, sigma, and pi electrons:

a. In organic molecules, one can predict from their UV and VIS spectra whether double bonds are conjugated; less energy is required to excite a pi electron in conjugated double bonds than in isolated double bonds because the energy difference between the highest occupied and the unoccupied molecular orbitals is less for conjugated than for isolated double bonds. Examples of trends of spectral changes (wavelength and molar absorptivities) due to structural changes are found in Chapter 5.

b. Transitions involving $n \rightarrow \pi^*$ are of lower energy than transitions from $n \rightarrow \sigma^*$ because π^* orbitals are of lower energy than the corresponding σ^* orbitals (Fessenden 1982; Atkins 1990).

c. Electronic transitions from $n \rightarrow \pi^*$ or $n \rightarrow \sigma^*$ are of lower molar absorptivities (less intense) than transitions from $\pi \rightarrow \pi^*$ or from $\sigma \rightarrow \sigma^*$ (about 1 percent) because the n electrons have a different orientation in space and therefore, according to the selection rules, their transitions are forbidden.

Figure 10 is a simplified molecular orbital diagram of acetone, $(CH_3)_2\ C = O$, summarizing the $n \rightarrow \pi^*$ and $\pi \rightarrow \pi^*$ transitions of the n electrons around the oxygen atom and the π electrons between the carbon and oxygen atoms in the carbonyl group, $C = O$. The diagram also shows the involvement of singlet and triplet states regardless of whether the particular transition is allowed.

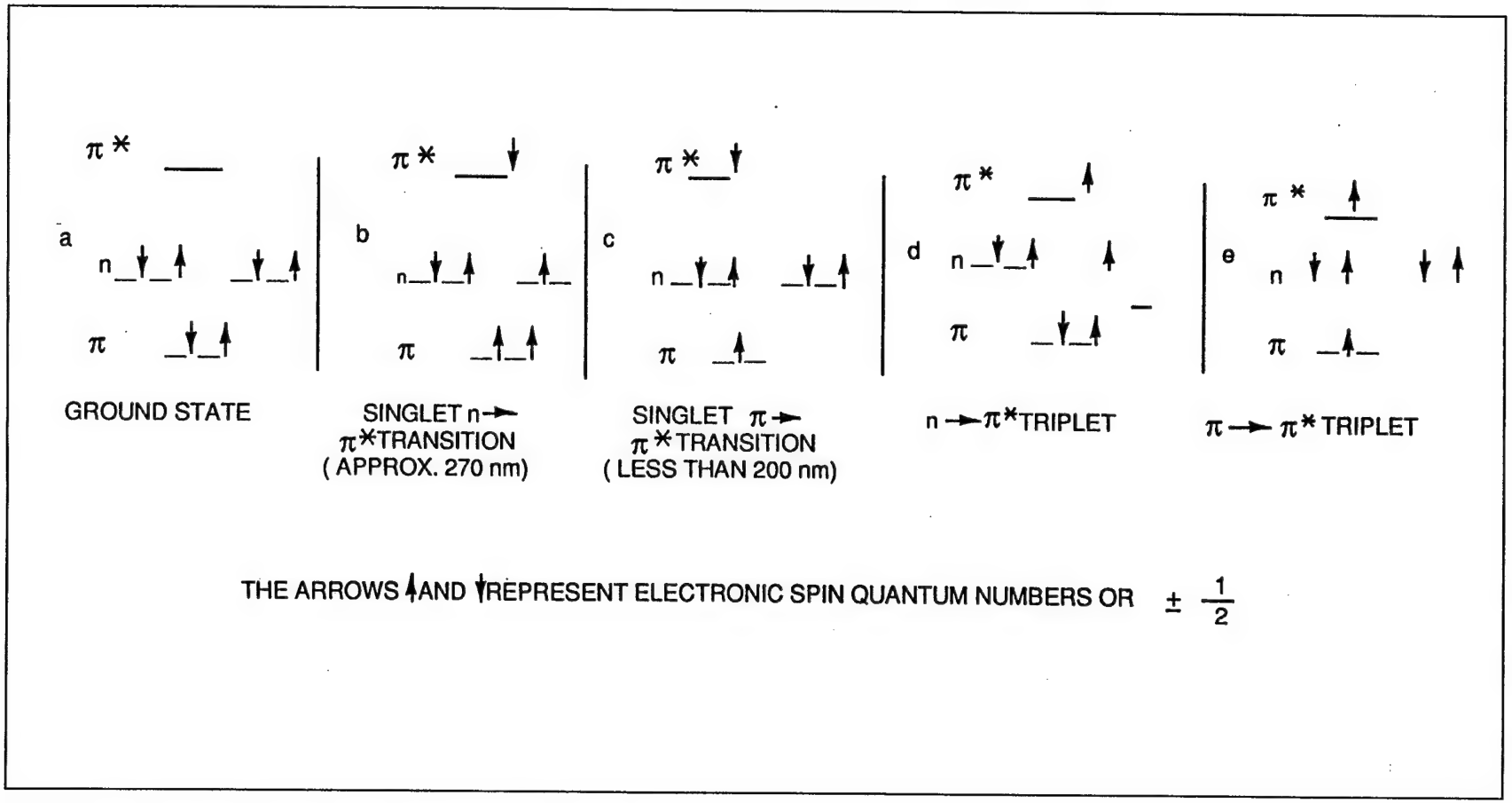

Figure 10. Simplified molecular orbital diagram of acetone

4 Vibrational and Rotational Excitations

Infrared Region

A photon in the IR region possesses less energy than a photon in the VIS or UV regions (2-15 kcal/mole compared to 40-300 kcal/mole in the UV and VIS regions). Near IR photons interact with the vibration of bonds between atoms in a molecule. A molecule can absorb IR if it forms an oscillating dipole moment which can interact with the electric field component of the IR and also if the vibrations of the molecule correspond to those of the IR vibrations. A molecule absorbs fixed but quantized vibrational energy, increasing the vibrational amplitude of its bonds and, thereby, acquiring excited vibrational states.

Two nuclei bonded covalently vibrate similarly to two balls attached by a spring. Double and triple bonds might be thought of as stronger springs. At equilibrium distance, a molecule's vibrational energy is minimum, and a diatomic molecule might be considered as being at the bottom of a potential energy well.

The average distance between the two atoms represents the covalent bond length prior to IR vibrational excitation. Different bonds or different functional groups absorb different but specific vibrational energies. For example, the O-H bond absorbs between 3,000 and 3,700 cm^{-1}, corresponding to wavelengths between 2.7 and 3.3 μm, whereas the C-O bond absorbs between 900 and 1,300 cm^{-1} or between 8 and 11 μm.

Also the same bond can absorb energy at more than one frequency or wave number, i.e., the reciprocal of the wavelength. The specific frequency of absorption depends on whether the bond is experiencing a stretching or a bending mode of vibration. For example, an O-H bond absorbs at 3,300 cm^{-1} (3.0 μm) due to its stretching vibrations, while the same O-H bond absorbs at 1,250 cm^{-1} (8.0 μm) due to its bending vibrations. Except where hydrogen bonding is involved, absorption bonds broaden, and intensity increases, infrared is insensitive as to whether the substance is gas, liquid, or solid.

The amplitude of the wavelength or the vibrational intensity is dependent on whether the particular vibrational excitation transition is or is not allowed, according to the various selection rules. The allowed vibrational energy for a particle, according to the selection rules, is given by the equation:

$$\in_{vib} = (\upsilon + \frac{1}{2}) \frac{h}{2\pi} \sqrt{\frac{k}{m}} \tag{41}$$

where

m = mass of the particle

k = force constant

υ = vibrational quantum number, which has an integral value such as 0, 1, 2, 3, etc. (Barrows 1981)

The above equation can also be written as $\in_{vib} = (\upsilon + \frac{1}{2}) h\nu$, since the frequency $\nu = \frac{1}{2\pi} \sqrt{\frac{k}{m}}$.

Another restriction on the vibrational quantum number is that $\Delta\upsilon = \pm 1$, which means that transitions are allowed only between vibrationally adjacent energy levels.

The uniqueness of IR spectra for each organic compound makes it a powerful tool for identification. Figure 11 shows the IR spectra of the example compounds, the *cis* and *trans* isomers of 2-(p-dimethylaminobenzylidene)-4-butyrolactone.

Fourier Transform Infrared Region (FTIR)

Due to innovative technology, IR and NMR dispersive spectrophotometers are being replaced by Fourier transform systems in which the resultant signal is an interferogram resulting from the sum of individual signals caused by each wavelength. Each point in the interferogram is a culmination of all frequencies in the spectrum. FTIR spectrophotometers are very fast and offer high resolution.

Figure 12 represents a simplified Michelson interferometer for the FTIR spectrophotometer, showing the source, beam splitter, fixed and moving mirror positions, sample holder, and detector.

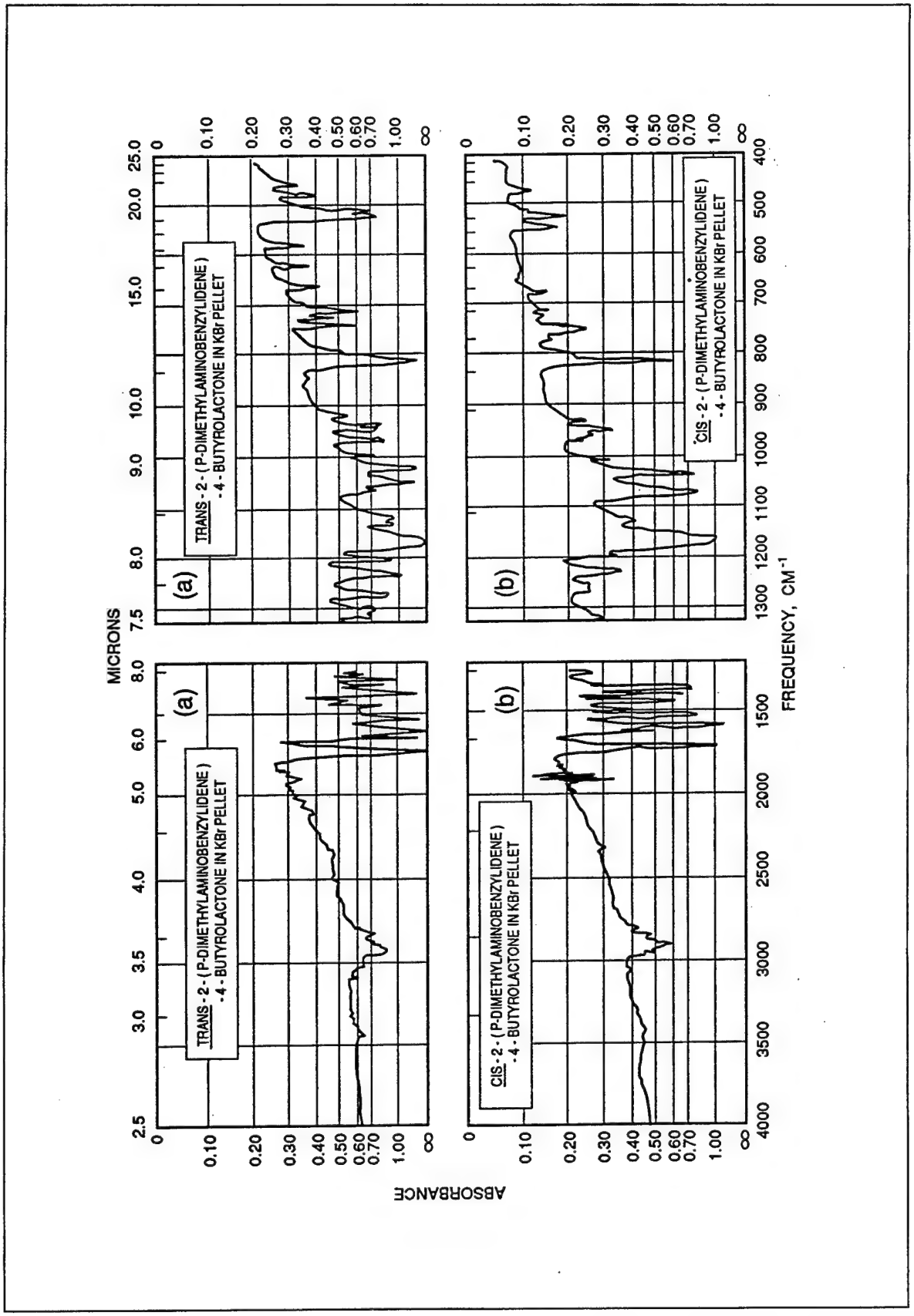

Figure 11. Sample IR spectra for *trans* and *cis* 2-(p-dimethylaminobenzylidene)-4-butyrolactone

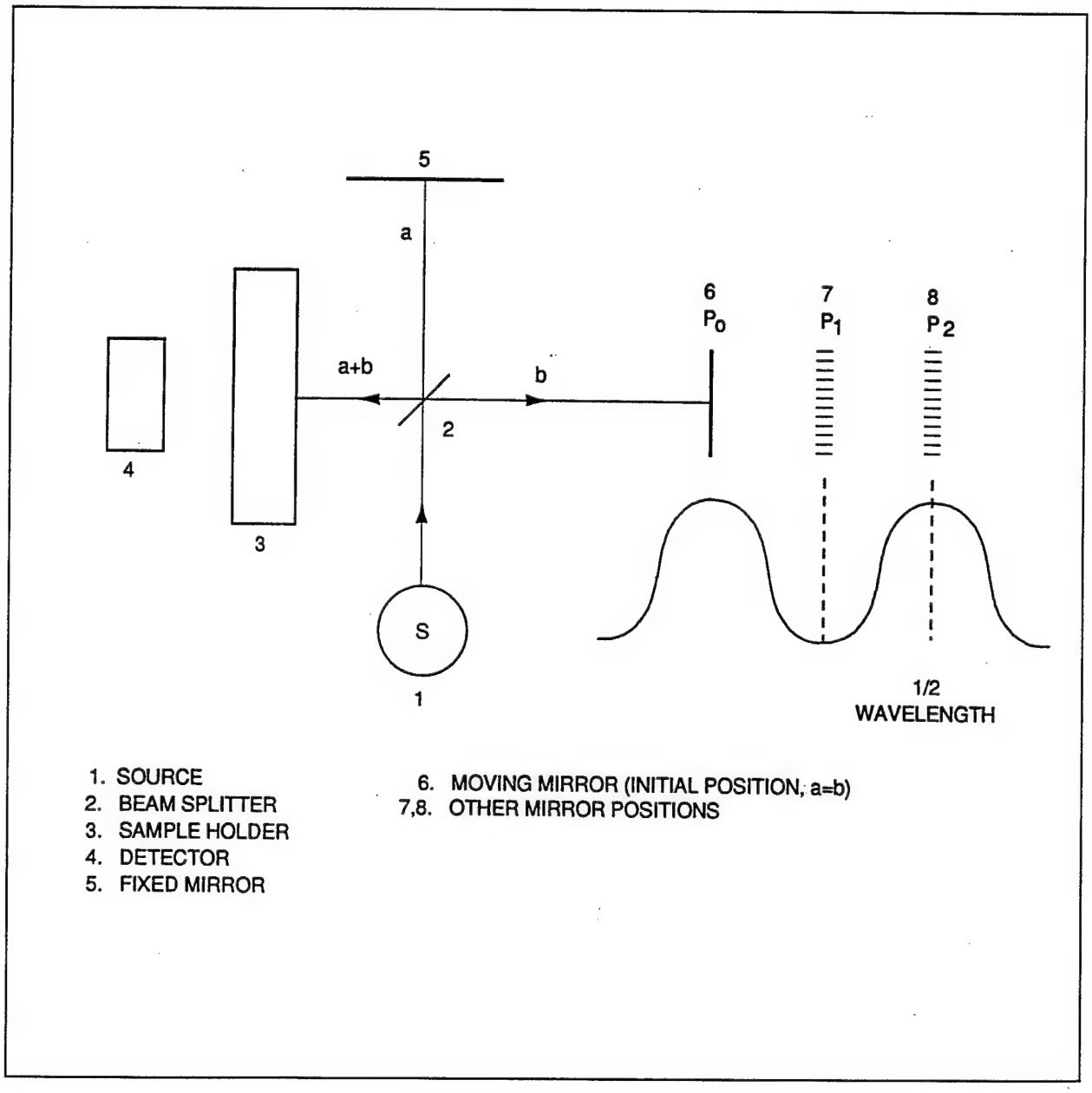

Figure 12. Michelson interferometer

Microwave

The microwave region of electronic radiation deals with the pure rotation of molecules and can be used for the measurement of bond lengths and molecular angles. The following are summary statements of angular momentum, selection rules for the allowed rotational states, and the quantized rotational energy states:

a. The total angular momentum, $I\omega$, must satisfy the equation

$$I\omega = \sqrt{J(J+1)}\,\frac{h}{2\pi} \tag{42}$$

where

rotational quantum number $J = 1, 2, 3$, etc.

ω = angular velocity

I = momentum of inertia

$$I = \sum m_i r_i^2 \tag{43}$$

where

m_i = mass of the particle

r_i = rotational radius

b. The vector component of the angular momentum in a direction imposed on the rotating particles by an electric or magnetic field is given by $M\,\frac{h}{2\pi}$

where

M = -J, -J+1, -J+2...0, 1..., J

c. Rotational transitions are allowed only between adjacent rotational energy levels, or

$$\Delta J = \pm 1 \tag{44}$$

d. Rotational energy is easily derived from the angular momentum and is given as

$$\in_{rot} = J(J+1)\,\frac{h^2}{8\pi^2}\,\frac{}{I} \quad \text{(Barrows 1981)} \tag{45}$$

Nuclear Magnetic Resonance (NMR)

When placed in a strong magnetic field, nuclei of atoms with magnetic resonance moments (atoms having odd atomic numbers or atomic masses, such as hydrogen and carbon -13) act as small magnets.

More than one-half of these nuclei align themselves with the magnetic field where they will be in their lowest spin states. Upon absorbing the needed radio frequencies, they will then align themselves against the field, going into a higher spin state. Transition to this higher energy state (magnetic resonance) depends on both the external magnetic field and on the nucleus nuclear magnetic moment.

Nuclear magnetic resonance is governed by the selectively allowed components of the nucleus angular momentum in the direction of the field and is summarized by the Equation 45. $\Delta E = h\nu = 2\mu H$, ν = frequency, μ = nuclear magnetic moment, H = field strength.

Since different nuclei in a molecule experience different environments due to different neighboring atoms, they therefore absorb different radio frequencies. In other words, one might say that resonance takes place at different frequencies or at different field strengths.

The separation of NMR signals, or the place where resonance occurs in the magnetic field as a result of atoms being in different environments, is called chemical shift and can be shown as:

$$\delta = \frac{H_{sample} - H_{reference} \times 10^6}{H_{reference}} \qquad (46)$$

where

H_{sample} and $H_{reference}$ = magnetic field strengths of the sample and reference compounds respectively (Barrows 1981)

The large single signal of the reference compound usually used—tetramethyl silane $(CH_3)_4$ Si, referred to as TMS—is assigned zero, H_z or zero parts per million (ppm) on the radio frequency scale. TMS is a convenient reference because its 12 protons are all in an identical environment and are shielded from the magnetic field by their electrons; protons in TMS do not have neighboring electronegative atoms which can deshield them by attracting the electrons toward themselves.

The more screened or shielded the protons are from the external magnetic field by their electrons, the larger (more upfield) the magnetic field needed to cause magnetic resonance, whereas the more protons are exposed or deshielded, the smaller (more downfield) the magnetic field needed to cause magnetic resonance.

Important structural information about molecules can be obtained from their proton NMR spectra.

For example:

a. The number of different environments (different sets of peaks) gives the number of the different kinds of hydrogen atoms in a compound.

b. The chemical shift, δ, gives information about the different environments and therefore about the different kinds of hydrogen atoms in a compound.

c. The relative integrated areas of the different groupings of chemical shifts reveal the relative number of hydrogen atoms in each group.

d. The spin-spin coupling pattern reveals the number of hydrogen nuclei in groups which interact with each other.

The *cis* and *trans* isomers of 2-(p-dimethylaminobenzylidene)-4-butyrolactone can be used to illustrate the previous points, showing how NMR techniques can be useful for structural determination. Figure 13 represents the NMR spectra of the *cis* and *trans* compounds, respectively. The molecular figures show arbitrary letter designations of the protons in different environments. Figure 13 shows definite assignments of spectra lines to protons in these two structures, giving their chemical shifts and coupling constants.

The singlet line of the six dimethylamino protons which are in the same environment is the most intense line of the spectrum and has about the same chemical shift for both isomers, 181 cps relative to TMS.

The lactone ring has two kinds of protons, B and M. The lines of the B protons for both isomers are partially buried under those of the A protons and are split into three sets of doublets by the adjacent lactonic protons, M, and by vinyl proton, Z. M is split into a triplet by B. As shown in Figure 13, the chemical shifts for B and M of the *cis* isomer are a few cycles upfield relative to TMS from those of the *trans* isomer.

The aromatic protons X and Y show two doublets, which approximate an X_2Y_2 pattern with the characteristic mirror image. X has the same chemical shift for both isomers. The chemical shift of Y is 34 cps further downfield for the *cis* than for the *trans* compound, where the Y protons are *cis* to the carboxylic oxygen and are therefore more deshielded than in the *trans* isomer, thus according for downfield shift.

The Z proton in both isomers is split into a triplet by B. The chemical shift for this proton is 36 cps further upfield for the *cis* isomer than for the *trans* isomer, because within the *cis* isomer the vinyl proton is *trans* to the carboxylic oxygen and is therefore less deshielded.

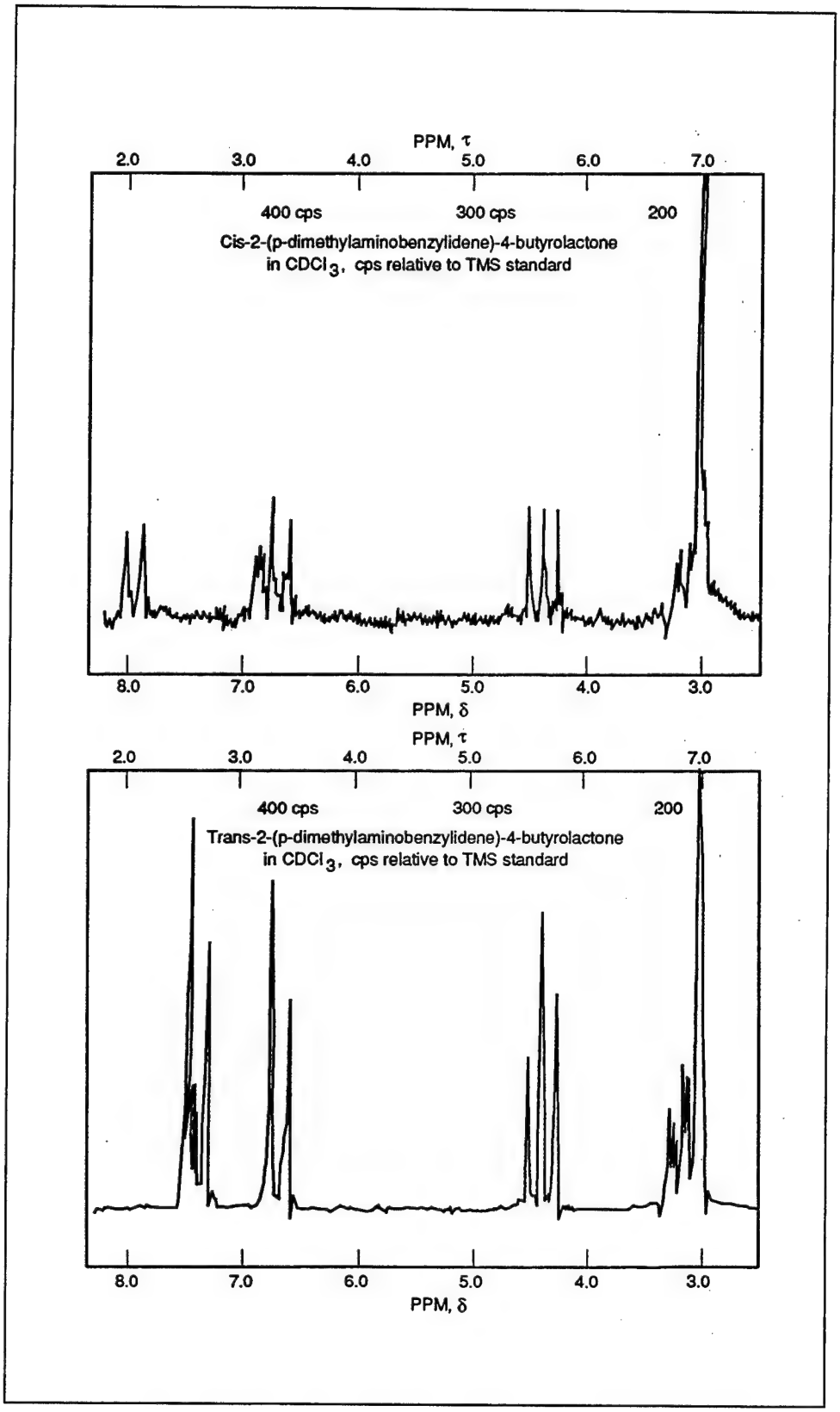

Figure 13. NMR spectra of the *cis-trans* isomers of 2-(p-dimethylamino-benzylidene)-4-butyrolactone

From these assignments, the structures of the *cis* and *trans* forms may be determined by the chemical shifts of the Y and Z protons in the two isomers.

Raman Spectra (Light Scattering)

Raman spectroscopy is the study of a small portion of light scattered by a molecule, the light undergoing an exchange of energy with that molecule. Unlike absorption and emission spectroscopy where the energy of a photon must correspond to the energy difference between two states of the molecule the photon interacts with, Raman scattering (change of direction) of the colliding photon can take place at any energy. The Raman effect emanates from the small fraction of scattered photons which undergo an increase or decrease in their energy due to their interaction with molecules. In contrast, the Rayleigh scattering effect describes the majority of photons, which scatter due to their collision with a molecule and do not undergo an exchange of energy with that molecule.

Raman shift is the difference of frequency in the photon before and after the scattering. The corresponding change of the photon energy is a measure of the energy spacing of the molecule. Since Raman scattered radiation is only about 10^{-5} (1 in 100,000) of the exciting radiation, a very intense monochromatic laser exciting beam is needed. As in emission spectroscopy, one observes Raman scattered radiation at a right angle to the incident beam.

In certain cases, Raman scattering becomes the only available tool to give information about a molecule. For example, unlike IR, Raman scattering offers information about nonspherical top, nonpolar molecules such as benzene, C_6H_6, and fluorine, F_2.

Raman vibrational spectroscopy can be more useful for molecules in aqueous systems since water shows only weak Raman scattering (between 300 and 3,000 per cm^{-1}) (Levine 1983). Raman scattering can be very informative as to hydrogen bonding in biological systems. Other examples of the usefulness of Raman scattering are, for instance, that it shows that carbonic acid is carbon dioxide dissolved in water rather than the associated acid, also that the mercurous ion is two single, positively charged ions, $Hg^+ - Hg^+$, rather than one, Hg^+.

5 Relationships Between Structural Changes in Molecules and Their UV and VIS (Wavelength and Molar Absorptivity) Spectra

For various organic compounds, it is desirable to predict the wavelengths of UV and VIS absorption maxima by correlating the spectra to changes in the structural chromophores of these compounds. This section will show a few representative examples. Although wavelengths of absorption are only approximate in some cases, they demonstrate definite trends.

Solvent Effects

Striking solvent effects were seen in our example of *cis-trans* 2-(p-dimethylaminobenzylidene)-4-butyrolactone in the polar and nonpolar solvents, alcohol and heptane, respectively. Generally, spectra in alcohol are used as a reference point. Spectra in water occur at about 8 nm longer than those in alcohol. Spectra in dichloroethane, tetrahydrofuran, diethyl ether and in heptane occur at about 2, 4, 7, and 11 nm, respectively—shorter than in alcohol. Therefore, it can be seen that spectra can be compared only within the same solvent system.

It can also be said that UV and VIS spectra show more hyperfine structural details in nonpolar than in polar solvents.

Extension of Conjugation of Polyenes and Similar Compounds

UV spectra show the presence of various chromophores such as conjugated systems and extent of conjugation. Generally the longer the conjugation, the

longer the wavelength of maximum absorption and also the higher the intensity. Too, (as shown by the addition of the alkyl groups) the more substituted the compounds, the longer the wavelengths of maximum absorption.

Alkenes and dienes without conjugated multiple bonds usually absorb light at wavelengths in the vacuum UV region (less than 200 nm). For example, ethene and 1,4-pentadiene absorb at 170 and 178 nm, respectively. Molecules with conjugated multiple bonds absorb at higher wavelengths than 200 nm. For example, 1,3-butadiene absorbs at 217 nm ($\in$ = 21,000).

When the number of conjugated double bonds increases, both the wavelengths of maximum absorbance and the intensity increase. This increase in wavelength is due to the lowering of energy caused by resonance stabilization. Each double bond addition increases the wavelength of maximum absorption between 30 and 35 nm; compounds with more than eight conjugated double bonds absorb in the VIS region. A comparison of the systems in Table 4 shows that extending the conjugation of polyenes increases the wavelength of maximum absorption.

Table 4
Conjugated Polyenes

Compound	Wavelength of Maximum Absorption, λ (nm approximate)	Moles Absorption, $\in_\lambda$ (approximate)
$H_2C = CH_2$ ethylene	170	15,550
$H_2C = CH - CH = CH_2$ 1,3-butadiene	217	20,900
$H_2C = CH - CH = CH - CH = CH_2$ *trans*-1,3,5-hexatriene	274	50,000
$H_2C = CH - CH = CH - CH = CH - CH = CH_2$ 1,3,5,7-octatriene	304	[1]
β-carotene (precursor of vitamin A) eleven conjugated double bonds	425 477	$\in_1 = 1.3 \times 10^5$
lycopene (red pigment of tomatoes) eleven conjugated double bonds	470 505	$.85 \times 10^5$

[1] Units of molar absorptively are $M^{-1}.Cm^{-1}$. However, these units generally are not given.

Polyenes Conjugated to Carbonyl Groups

Spectra of conjugated polyenes to carbonyl groups (in addition to the $n \rightarrow \pi^*$ transition, which occurs at longer wavelengths, generally with lower molar

absorptivities) have $\pi \rightarrow \pi^*$ transitions similar to those of conjugated polyenes in which both wavelengths and molar absorptivities increase with increase of the extent of conjugation. Also, comparing the following polyene-aldehyde structures show that the extent of the increase of wavelength becomes slower upon increasing the length of the conjugation (Table 5).

Table 5
Comparison of Polyene-aldehyde Structures

Compound	Wavelengths
$CH_3 - (CH = CH)_1 - CH = O$	λ = 220 nm
$CH_3 - (CH = CH)_2 - CH = O$	λ = 270 nm
$CH_3 - (CH = CH)_4 - CH = O$	λ = 343 nm
$CH_3 - (CH = CH)_5 - CH = O$	λ = 370 nm
$CH_3 - (CH = CH)_7 - CH = O$	λ = 415 nm

Branching and Methyl Group Substitution of Conjugated Polyenes and Similar Compounds

A comparison of the conjugated polyene system in Table 6 shows that, because of hyperconjugation of the sigma orbitals with the pi orbitals, the

Table 6
Conjugated Polyene Systems with Addition of a Methyl Group

Compound	Wavelength
$H_2C = CH - CH = CH_2$ 1,3-butadiene	λ = 217 nm $\in$ = 20,900
$H_2C = C(CH_3) - CH = CH_2$ 2-methyl-1,3-butadiene	$_1\lambda$ = 220 nm
$H_2C = CH - CH = CH - CH_3$ 1,3-pentadiene	λ = 223 nm $\in$ = 24,000
$CH_2 = C(CH_3) - C(CH_3) = CH_2$ 2,3-dimethyl-1,3-butadiene	$_1\lambda$ = 226 nm
$CH_3 - CH = CH - CH = CH - CH_3$ 2,5-hexadiene	$_1\lambda$ = 227 nm
1,3-cyclopentadiene	λ = 239 nm $\in$ = 34,000
$(CH_3)_2 C = CH - CH = C(CH_3)_2$ 2,5-dimethyl-2,4-hexadiene	λ = 244 nm $\in$ = 24,500
1,3-cyclohexadiene	$_1\lambda$ = 256 nm

[1] Units of $\in$, molar absorptivities, generally are not given.

addition of a methyl group increases the wavelength of absorption by approximately 4 to 6 nm.

Increase in the wavelengths of maximum absorption because of hyperconjugation of the methyl group's sigma orbitals with pi orbitals (conjugated carbon-carbon to carbon-oxygen pi system) are illustrated by the structures in Table 7.

Table 7
Increase in Wavelengths of Maximum Absorption[1]

Compound	λ(nm)	
$H_2C=CH-C(=O)-CH_3$ **3-buten-2-one**	$\pi\rightarrow\pi^1$(219) $n\rightarrow\pi^1$(305)	(Note: the $n\rightarrow\pi^1$ is a forbidden transition)
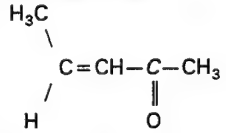 **3-penten-2-one**	$\pi\rightarrow\pi^1$(222) $n\rightarrow\pi^1$(311)	1,300 37
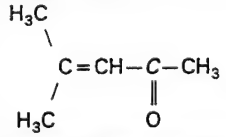 **4-methyl-3-penten-2-one**	$\pi\rightarrow\pi^1$(236) $n\rightarrow\pi^1$(314)	1,200 58

[1] Due to hyperconjugation of methyl group's sigma orbitals with conjugated pi systems.

This trend of increase in wavelength and in molar absorptivities (because of increases in conjugation of the pi system and the substitution of alkyl groups) can be clearly seen when the spectra of the above compounds are compared to that of the unconjugated parent compound, acetone:

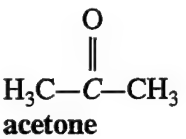
acetone
279 nm
189 nm

$\pi\rightarrow\pi^1$, λ = 189 nm ϵ = 900
$n\rightarrow\pi^1$, λ = 273 n ϵ = 15

Polycyclic Aromatic Compounds

Extension of polynuclear rings increases the wavelength of maximum absorption. For example, benzene, naphthalene, anthracene, tetracene, and pentacene have corresponding absorbencies at 200, 221, 252, 275, and 310 nm, respectively. Other wavelengths of absorbencies are shown in Table 8.

Table 8
Increase in Wavelengths of Maximum Absorption with Increase in Size of Aromatic Rings

Benzene, λ(nm) 	Naphthalene, λ(nm)	Anthrqcene, λ(nm)	Tetracene, λ(nm) 	Pentacene, λ(nm) 
180 (∈ = 60,000)	--	218	--	--
200 (∈ = 8,000)	221	258	275	310 (∈ = 251,200)
254 (∈ = 212)	275	295	--	--
261	286	310	--	--
268	311 (∈ = 239)	324	--	--
--	--	340	396 (∈ = 2,240)	--
--	--	357	418	--
--	--	376	446 (∈ = 8,130)	--
--	--	--	476 (∈ = 9,550)	575 (∈ = 12,600)

Note: Table 8 shows the maxima of representative wavelengths of similar electronic transitions but does not include all wavelengths of maximum absorption. (For example, benzene has other absorption maxima at 234, 239, 244, and 247 nm.

Extending the number of fused benzene rings is, in effect, an extension of the conjugated system. This lowers the difference between the $\pi \rightarrow \pi^1$ energy levels, which shows as longer wavelengths of maximum absorption.

Interactions Between n Electrons of the Side Chain and π Electrons of Aromatic Compounds

Strong interactions between n electrons of the side chain and π electrons of the aromatic ring lower the differences in energy levels, thereby exhibiting longer wavelengths of maximum absorption. This effect is similar to the lowering of energy due to extension of the conjugation of the π system.

Figure 14 shows this effect: compounds in the left column have more interaction between the n electrons of the side chain and the π electrons of the aromatic ring, whereas those in the right column do not possess as much $n \rightarrow \pi$ interaction.

Methyl Substitutions on the Benzene Ring

Table 9 shows two opposing trends. One effect is that the addition of more methyl groups on the benzene ring inductively increases the wavelengths of maximum absorption; the other is that this same increase in the number of methyl groups on the aromatic ring causes steric instability (which raises the energy/lowers the wavelengths of maximum absorption). Note that this table does not include all methyl substituted benzenes or all the electronic transitions of the same compound, but it does contain wavelengths for similar transitions. For example, benzene also has a $\pi \rightarrow \pi^*$ transition at $\lambda = 180$ nm ($\in = 55{,}000$) and at $\lambda = 200$ nm ($\in = 8{,}000$), while toluene has a similar transition at $\lambda = 189$ nm ($\in = 55{,}000$) and also at $\lambda = 208$ nm ($\in = 79{,}000$).

These two effects caused by the addition of methyl groups can be explained as follows: methyl and other alkyl substitutions on the benzene ring increase the wavelength of maximum absorption because of the interaction of the sigma electrons of the methyl groups with the π electrons of the aromatic ring, thus causing an inductive activation of the aromatic π system and a lowering of energy (more stability). However, because of the steric effect caused by high methyl substitutions, part of this gained stability is lost when the compounds are highly substituted as in the case of penta- and hexamethyl benzenes. This loss of stability, which manifests itself as an increase in energy (a lowering of the wavelength), is due to steric interference created by the methyl groups around the aromatic ring. It is worth noting from Table 9 that p-xylene is more stable than 0-xylene (longer wavelengths), because the methyl groups in p-xylene are far apart and less sterically hindered. This table also shows that

maximum stability is achieved in 1,2,4,5-tetramethylbenzene, where inductive stability is more important than steric effect.

Chlorosubstituted Benzenes

Table 10 is a list of the most significant wavelengths of maximum absorption of chloro substituted benzenes. Generally, the more chlorine substituted, the longer the wavelength. This is caused by a lowering of energy due to the stabilization gained by extension of the conjugated system by the n electrons on the chlorine atoms. These wavelengths represent a compromise between this conjugation extension effect and two opposing effects, one caused by the electron-withdrawing inductive effect due to electronegativity of the chlorine atoms and the other due to the steric effect caused by high substitution of chlorine atoms on the plane of the benzene ring.

Di- and Trinitrobenzenes and Toulenes

Figure 15 shows various structures of di- and trinitrobenzenes with their respective wavelengths of maximum absorption. These wavelengths represent the weighted results of the resonance, inductive, and steric effects. As expected, dinitrobenzenes (which are less sterically hindered and which have one less

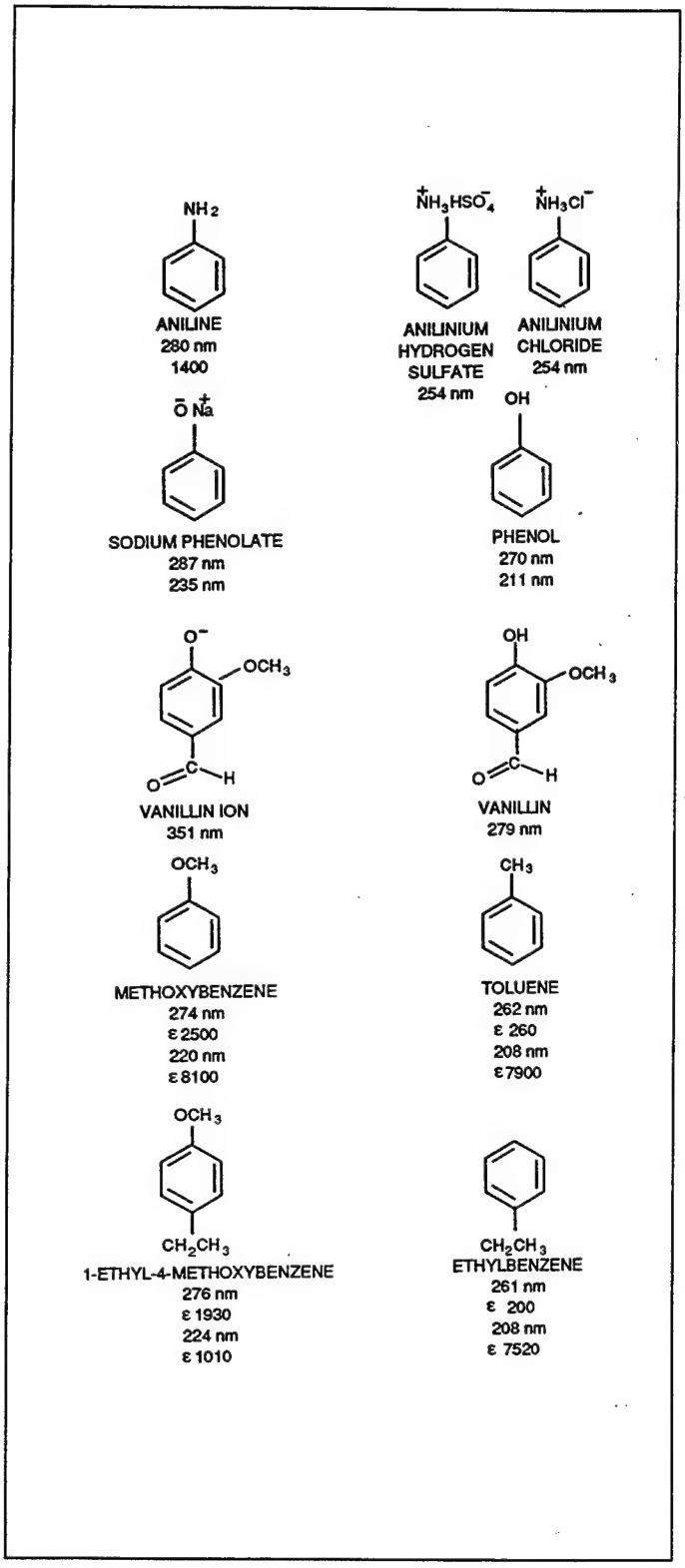

Figure 14. Effect of interaction between π electrons of the aromatic ring and n electrons of the side chain

Table 9
Effect of Addition of Methyl Groups on the Benzene Ring

EFFECT OF ADDITION OF METHYL GROUPS ON THE BENZENE RING

BENZENE

λ = 254 nm
ε = 212

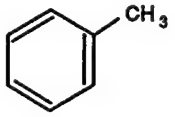

TOLUENE

λ = 262 nm
ε = 280

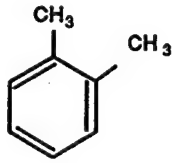

O-XYLENE

λ = 263 nm
ε = 160
λ = 273 nm
ε = 230

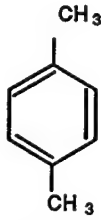

P-XYLENE

λ = 267 nm
ε = 500
λ = 275 nm
ε = 500

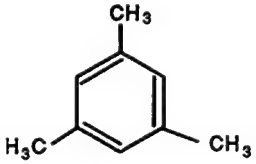

1,3,5-TRIMETHYL-BENZENE

λ = 267 nm
ε = 220
λ = 273 nm
ε = 230

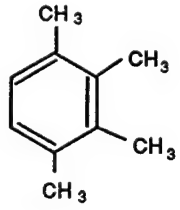

1,2,3,4-TETRAMETHYL-BENZENE

λ = 268 nm
ε = 316
λ = 273 nm
ε = 250
λ = 276 nm
ε = 250

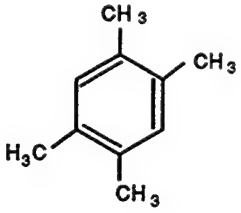

1,2,4,5-TETRAMETHYL-BENZENE

λ = 268 nm
ε = 630
λ = 272 nm
ε = 630
λ = 278 nm
ε = 638

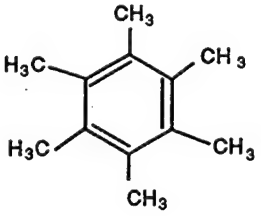

HEXAMETHYL BENZENE

λ = 275 nm
ε = 190

Table 10
Wavelength and Structural Variations of Chlorosubstituted Benzenes

Compound	Wavelength, nm
Chlorobenzene	245, 251, 258, 264, 272
1,2-dichlorobenzene	250, 256, 263, 270, 277
1,3-dichlorobenzene	250, 256, 263, 270, 278
1,4-dichlorobenzene[1]	258, 266, 273, 280
1,2,3-trichlorobenzene	265, 273, 280, (285)
1,2,4-trichlorobenzene	270, 278, 287
1,3,5-trichlorobenzene[2]	273, 285, 294
1,2,3,4-tetrachlorobenzene	274, 280, 291
1,2,3,5-tetrachlorobenzene	274, 281, (290)
1,2,4,5-tetrachlorobenzene[3]	276, 285, 294
Pentachlorobenzene	288, 289
Hexachlorobenzene	291, 301

[1] Least steric hindrance of the three dichlorobenzenes, therefore the most stable (longest wavelength).
[2] Least steric hindrance of the three trichlorobenzenes, therefore the most stable (longest wavelength).
[3] Least steric hindrance of the three tetrachlorobenzenes, therefore the most stable (longest wavelength).

electron-withdrawing nitro group than trinitrobenzenes) are of lower energies; their absorption wavelengths are longer. Also, a comparison of the three dinitrobenzenes shows the 1,4- and 1,2-dinitrobenzenes to be the most and the least stable, respectively (the compounds with the lowest energy/longest wavelengths and the highest energy/shortest wavelength, respectively). This is because 1,4-dinitrobenzene is the least sterically hindered. The most sterically hindered is 1,2-dinitrobenzene, because the two nitro groups interfere with each other in the plane of the aromatic ring.

A comparison of wavelengths of maximum absorption of dinitrotoluene to those of corresponding structures of trinitrotoluenes shows that dinitrotoluenes absorb at longer wavelengths and also, for both di- and trinitrotoluenes, the compounds which are less sterically hindered absorb at longer wavelengths (less energy). These wavelengths, shown in Figure 16 are the results of the resonance, inductive, and steric effects.

Most deactivation of the aromatic ring occurs when both nitro groups are ortho (on both sides) to the substituted group. In this case, all three effects: resonance, inductive, and steric are very strong. Nitro groups in the para position have the same resonance deactivation effect as those in the ortho

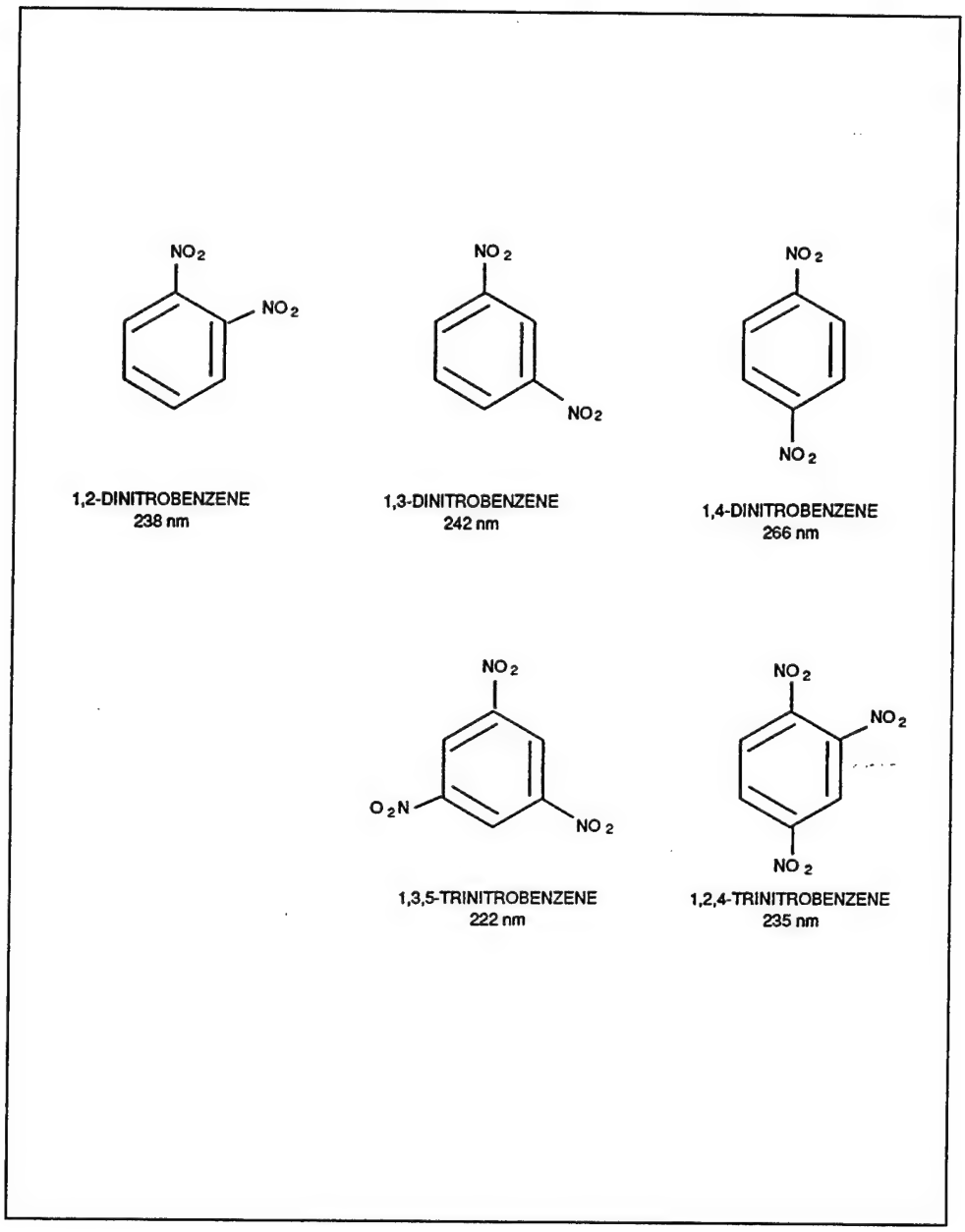

Figure 15. Wavelengths of maximum absorption and structural variations of di- and trinitrobenzenes

position; however, their inductive deactivation effect is less. Their steric destabilization is also less than that of the nitro groups adjacent to the methyl group (ortho position). Nitro groups meta to the methyl group have the least resonance deactivation effect.

Upon addition of potassium hydroxide and sodium sulfite in acetone medium, di- and trinitrobenzenes and toluenes absorb light in the visible region. The absorption of light at these long wavelengths is due to the

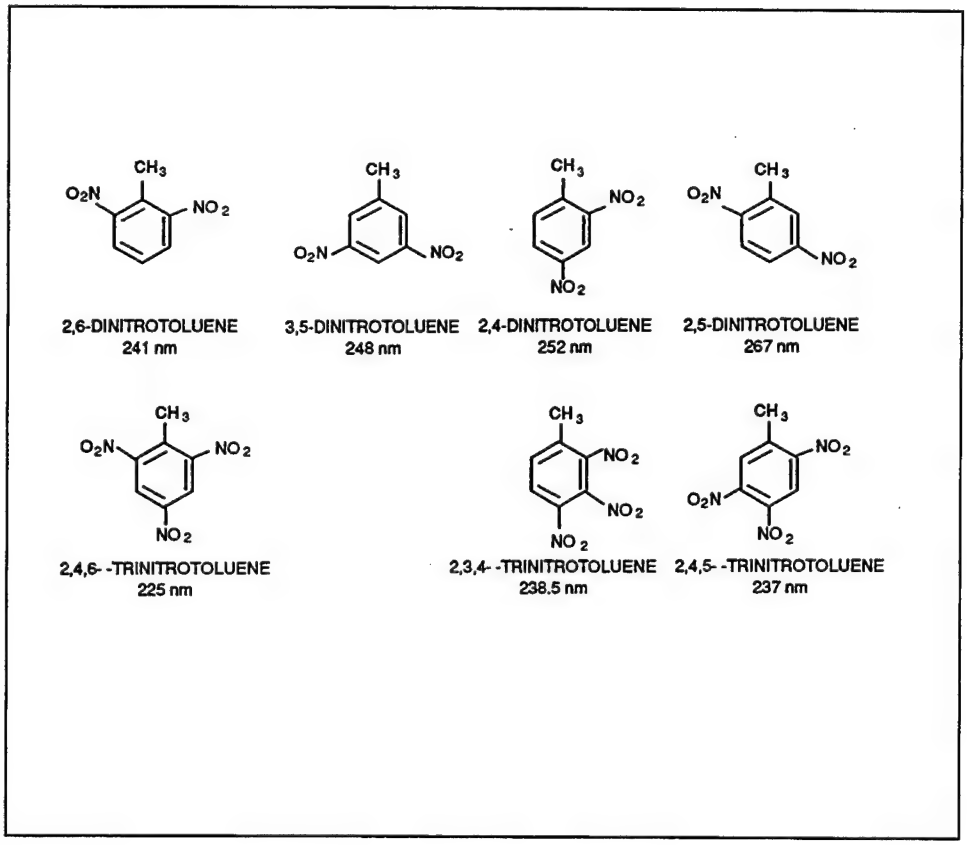

Figure 16. A comparison of wavelengths of maximum absorption of dinitrotoluenes with corresponding trinitrotoluenes

formation of Meisenheimer anion intermediates, which are stabilized by the electron-withdrawing nitro groups. These colored intermediates are formed only by additions of nucleophiles such as SO_3^{-2}, OH, and OCH_3 anions to positions ortho or para to electron-withdrawing substituents such as NO_2. These colored anions exhibit similar relationships of wavelengths to structural variations as those of the parent compounds (except at much longer wavelengths): dinitrosubstituted and other less sterically hindered anions absorb at longer wavelengths than trinitrosubstituted and more sterically hindered anions (Figure 17).

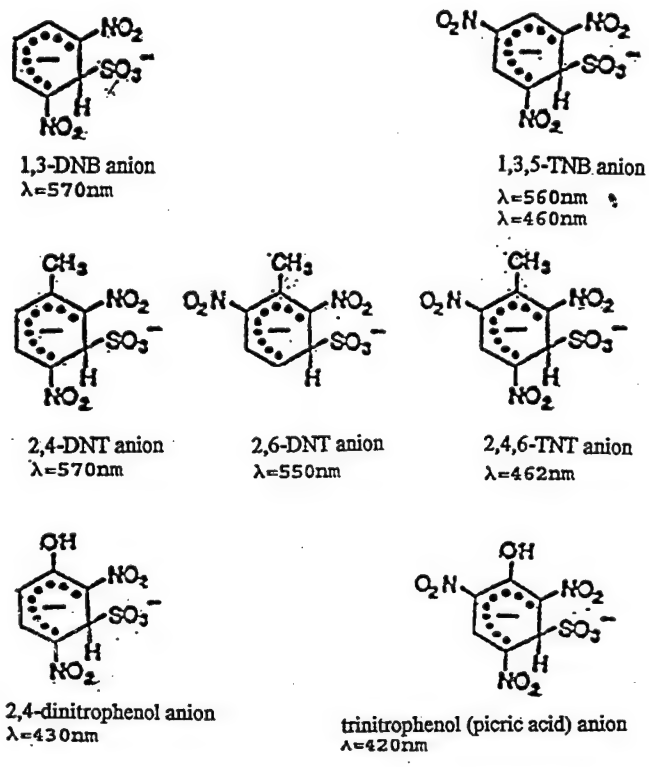

Note: Dinitrosubstituted aromatic anions absorb as longer wavelengths than trinitrosubstituted aromatic anions. Also, the less sterically hindered are these anions, the longer the wavelengths of maximum absorption. For example, the less sterically hindered sulfite anion, 2,4-DNT, absorbs at 570 nm, whereas, the more sterically hindered sulfite anion of 2,6-DNT absorbs at 550 nm.

Figure 17. Relationships of wavelengths and structural differences in sulfite anions of di and trinitrobenzenes and toluenes

6 Examples of Applications of UV and VIS Spectroscopy to Organic Molecules

Use of UV and VIS Spectra to Study Organic Molecules

In order for a molecule to interact with electromagnetic radiation and for changes in a molecule to take place, the molecule's natural frequencies must match those of the electromagnetic radiation. It is therefore necessary for a molecule to absorb energy at a particular frequency for a change to be affected, even though electromagnetic radiation which is not absorbed by a molecule may indirectly induce emission (First law of photochemistry (Alberty 1983)).

Consider, for instance, the example compound *cis-trans* photochemical isomerization of 2-(p-dimethylaminobenzylidene)-4-butyrolactone illustrating the effect of selective irradiation at 10 wavelength increments between 400 and 330 nm in the polar and nonpolar solvents, ethanol and heptance, respectively.

Striking solvent effects were observed in the absorption spectra. In nonpolar solvents, the most intense $\pi \rightarrow \pi^*$ band shifts hypsochromically (relative to polar solvents) and splits into two separate maxima, possibly due to vibrational structure, Figure 18.

The photostationary concentration ratios and the quantum yields for photochemical *cis-trans* interconversion were determined (Tables 2 and 3).

Figures 19 and 20 show representative spectra resulting from irradiation at 370 and 300 nm in heptane; and 390 and 330 nm in ethanol, respectively. These figures show that the photostationary state of the two isomers is approached from both directions, *cis* → *trans* and *trans* → *cis*.

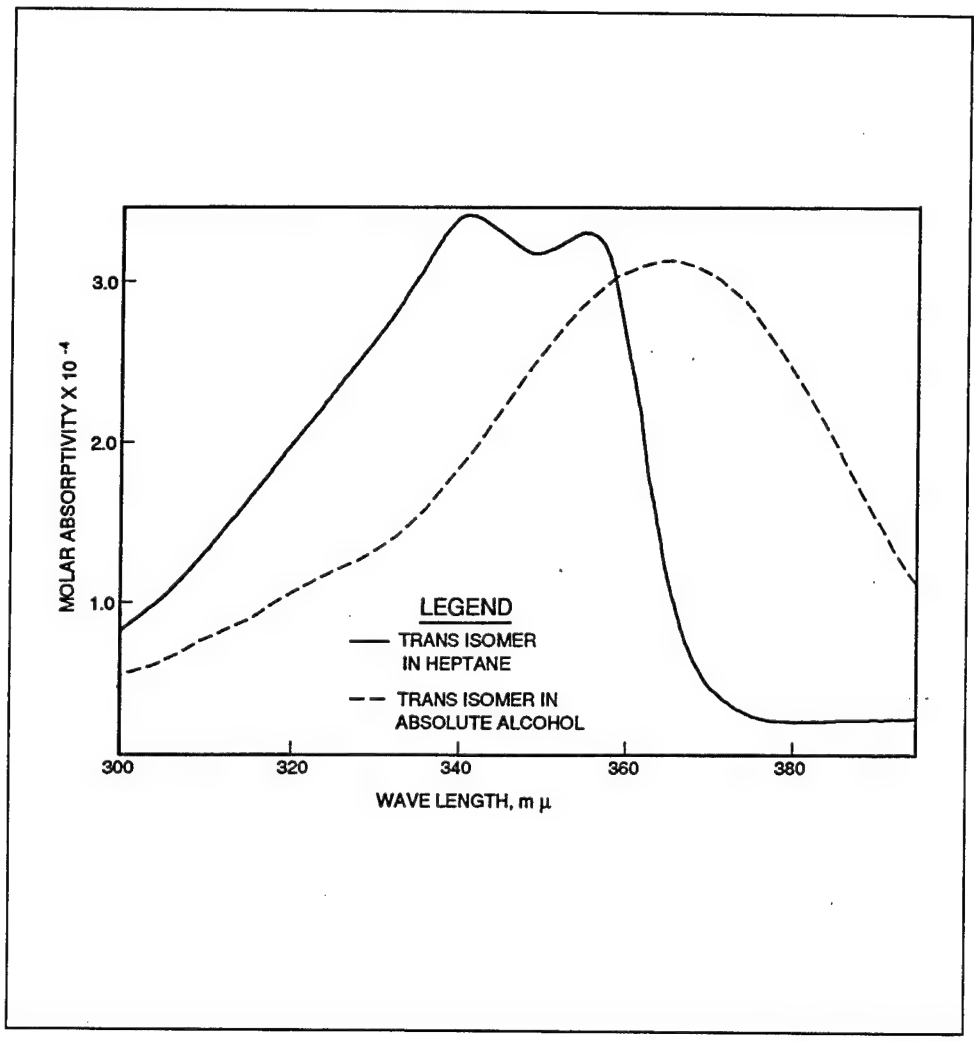

Figure 18. Absorption spectra of *trans* 2-(p-dimethylaminobenzylidene)-4-butyrolactone

Figure 21 and Table 11 show the photostationary concentration ratios at all wavelengths of irradiation (from 400 to 330 nm).

A dramatic example of the first law of photochemistry (that no absorption of light results in no change) is of the complete conversion of the *cis* to the *trans* isomer when the *cis* isomer is irradiated at 380 nm in heptane—where the *trans* isomer does not absorb. Because the *trans* isomer does not absorb light at this wavelength, a complete photochemical conversion of the *cis* to the *trans* isomer occurs at the photostationary state (equilibrium) (Figure 22). Since the concentration of the *trans* isomer formed by this complete photochemical conversion is the same as that of the *cis* isomer before irradiation and since the concentration of the *trans* isomer can easily be obtained by comparison with a standard solution of the *trans* isomer (using Lambert-Beer's law: absorbance is directly proportional to concentration or $A = \in cl$),

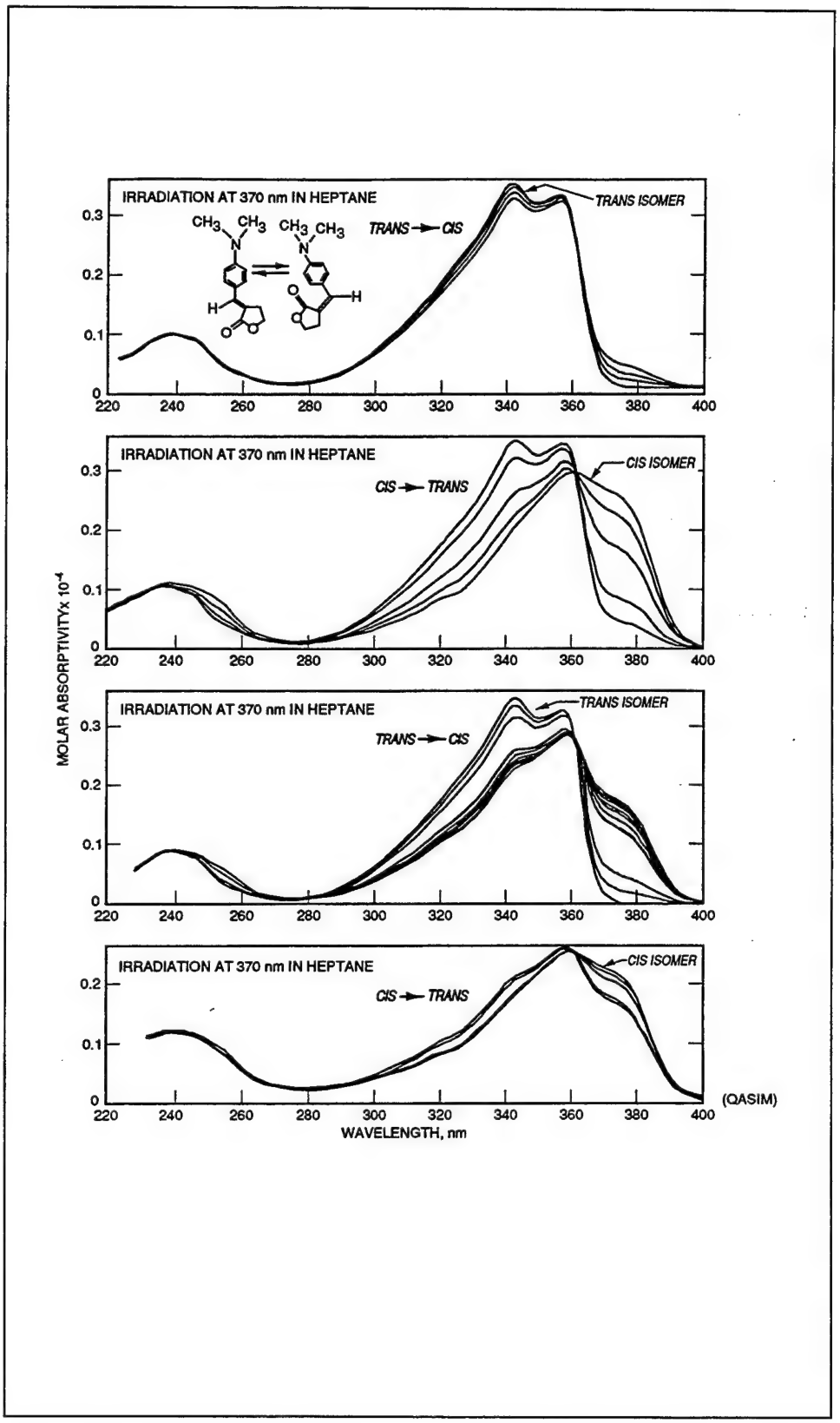

Figure 19. Representative spectra of 2-(p-dimethylaminobenzylidene-4-butyrolactone in heptane

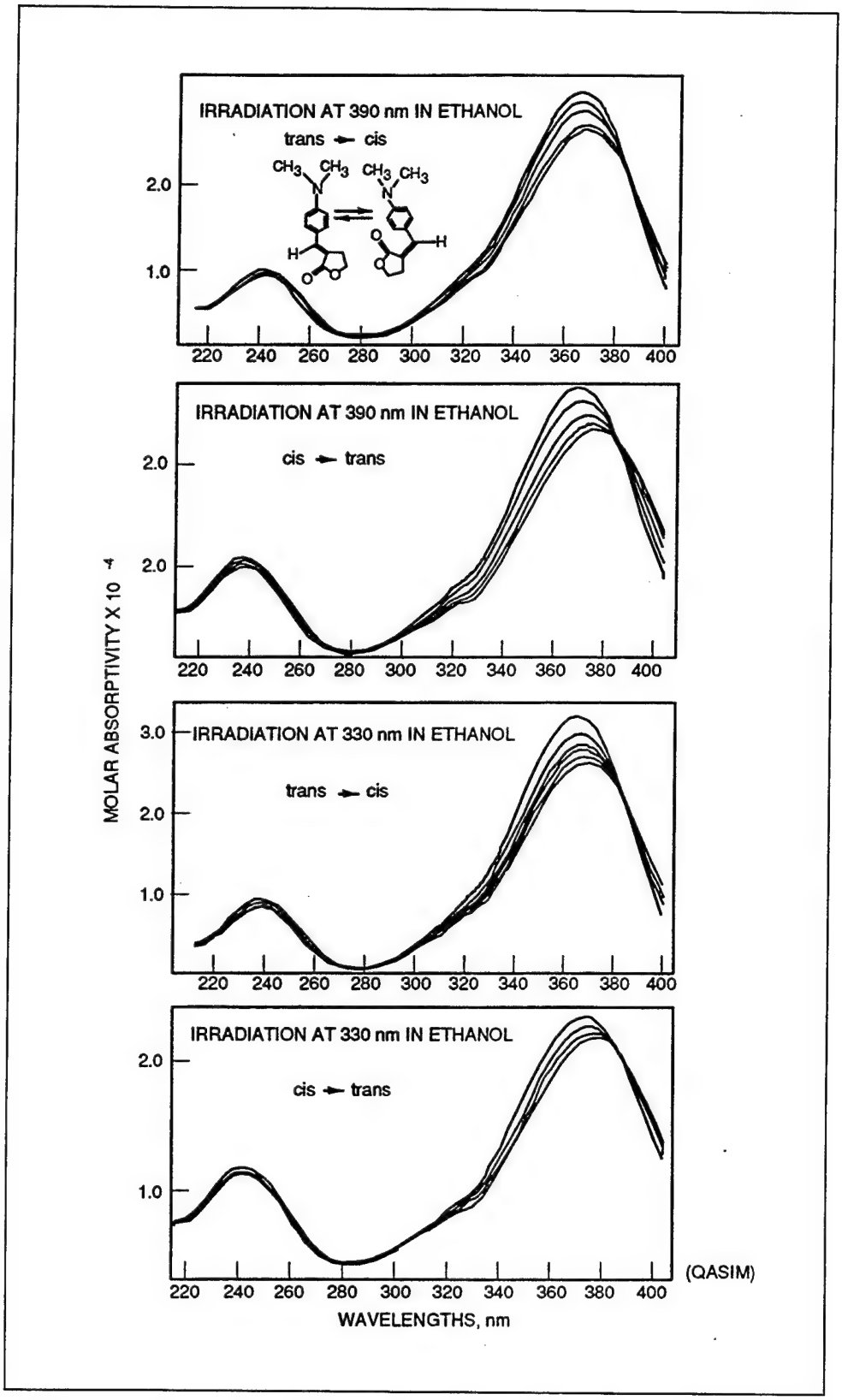

Figure 20. Representative spectra of 2-(p-dimethylaminobenzylidene-4-butyrolactone in ethanol

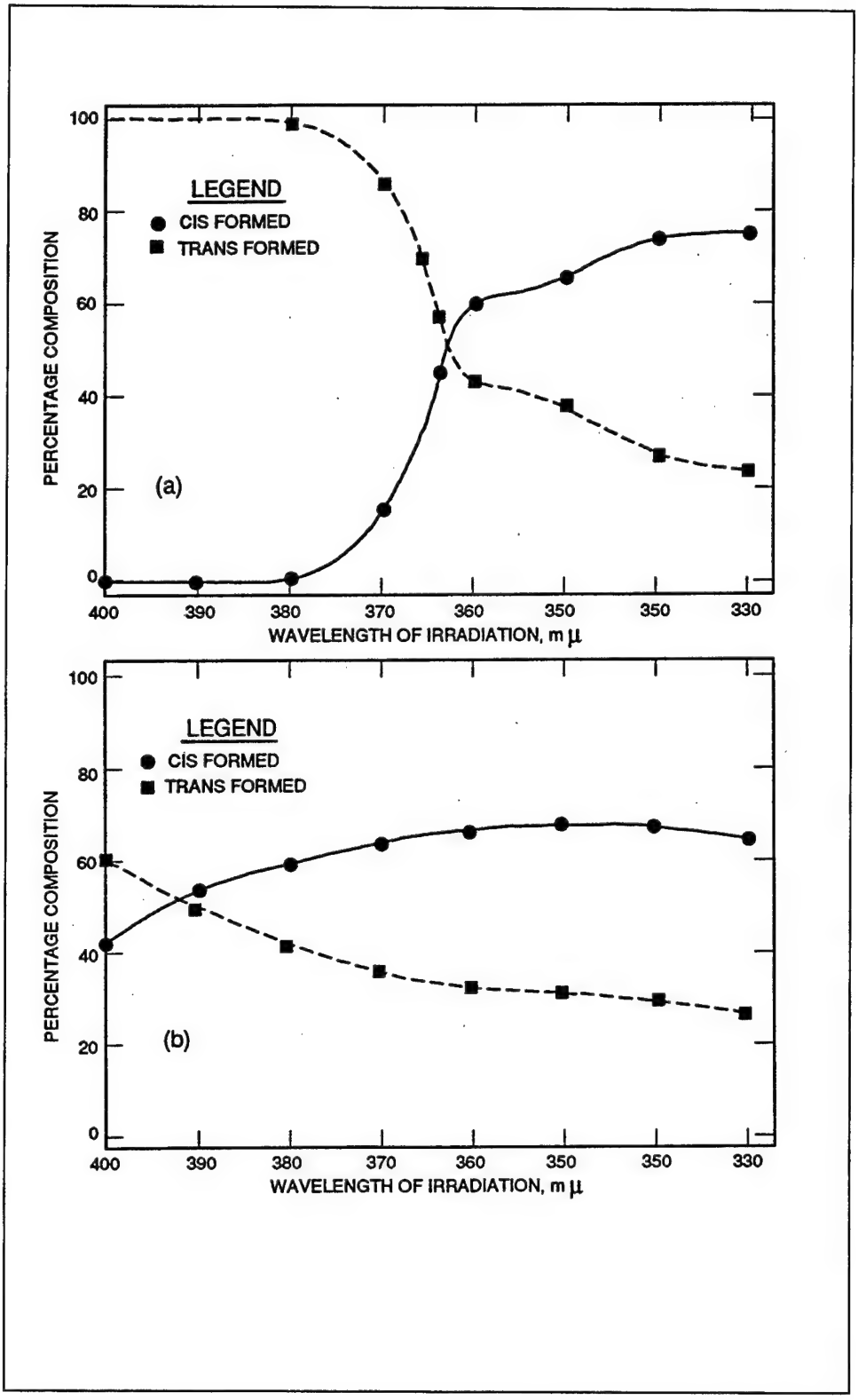

Figure 21. Photostationary concentration ratios at wavelengths from 400 to 330 nm

Table 11
Photostationary Composition of *cis-trans* Isomers of 2-(p-dimethylaminobenzylidene)-4-butyrolactone at Various Wavelengths of Irradiation

The Photostationary Composition of cis and trans-2-(p-dimethylaminobenzylidene)-4-butyrolactone at the various wavelengths of irradiation.

	Heptane System					
	t ⟶ c			c ⟶ t		
λ, nm	% c	% t	% t / % c	% c	% t	% t / % c
370	15.91	84.09	5.29	13.55	86.45	6.38
360	59.99	40.01	0.67	56.90	43.10	0.76
350	65.87	34.13	0.52	62.38	37.62	0.60
340	73.66	26.34	0.36	72.39	27.61	0.38
330	74.97	25.03	0.33	76.60	23.40	0.31
	Absolute Alcohol System					
400	44.38	58.62	1.42	38.76	61.24	1.58
390	54.26	45.74	0.84	49.69	50.31	1.01
380	59.36	40.64	0.69	57.36	42.64	0.74
370	64.09	35.91	0.56	63.89	36.11	0.57
360	66.70	33.30	0.50	66.71	33.29	0.50
350	67.65	32.35	0.48	68.49	31.51	0.46
340	67.20	32.80	0.49	70.09	29.91	0.43
330	64.24*	35.76*	0.56*	73.37	26.63	0.36

*Photostationary state was not completely attained.

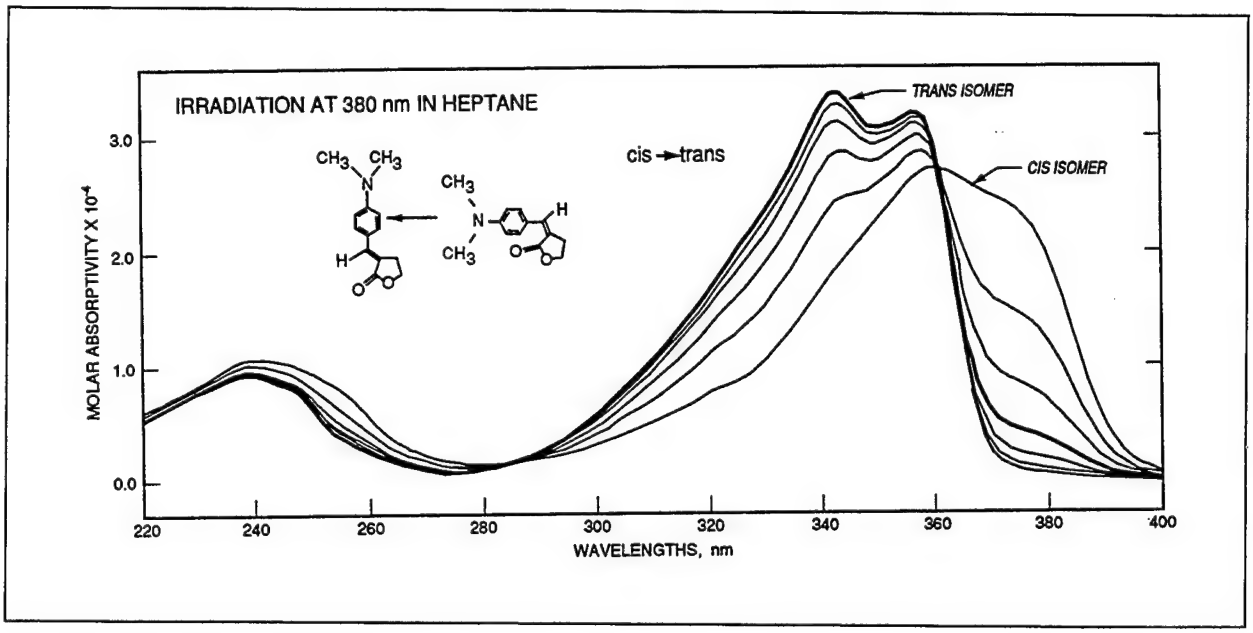

Figure 22. Comparison of molar absorptivities of both isomers at wavelengths from 400 to 300 nm

complete conversion of the *cis* to the *trans* isomer at this wavelength of irradiation, 380 nm, (where the *trans* isomer does not react with electromagnetic radiation—does not absorb light) provides a method for measuring small concentrations of the *cis* isomer that cannot otherwise be attained.

Figure 22 also provides a direct comparison of the molar absorptivities of the two isomers from 400 to 300 in the UV spectral region.

Example of Use of Emission Spectra to Investigate Nature of Excited States for 2-(p-dimethylamino-benzylidene)-4-butyrolactone

With the sample compound, 2-(p-dimethylaminobenzylidene)-4-butyrolactone, the emission spectra of the *cis* isomer in ethanol (EA) and in methylcyclohexane isopentane (MCIP), 1:1, resulted from irradiation at 313 and 366 nm and formed mirror images with the absorption spectra probably indicating fluorescence from the lowest vibrational level of the first excited state to the ground state. The 0-0 band energies of both isomers appeared to be of equal magnitude, 70 kcal.

The delayed emission of the *cis* isomer in EA and in MCIP and also of the *trans* isomer in EA resulted only from excitation at 313 nm, unlike the fluorescence caused by excitation at both 313 and 366 nm. However, the delayed emission was identical to that of the fluorescence in shape and energy. Therefore the slow emission of the *cis* isomer in EA and in MCIP and of the *trans* isomer in EA can be attributed to delayed fluorescence emitted from the first

singlet excited state. At least one triplet and probably higher excited singlet states were involved.

The long wavelength emission of the *trans* isomer in MCIP, unlike other delayed emission, can not be induced by excitation at both 313 and 366 nm but also differs in not forming a mirror image relationship with the absorption spectrum (Figure 7).

The reason for the *trans* isomer showing delayed fluorescence in EA and probably phosphorescence in MCIP suggests that, in nonpolar solvents, phosphorescence from the triplet to the ground state is preferred energetically to deactivation via the excited singlet state (delayed fluorescence). Delayed fluorescence in polar solvents could be due to intersystem crossing from the triplet to the excited singlet state or to triplet-triplet annihilation. However, the comparatively long mean decay time of the emitting species probably indicates the involvement of intersystem crossing.

Information regarding the mechanisms in both polar and nonpolar solvents are represented in the following Jablonski diagram, Figure 23. The straight and wavy arrows in these diagrams represent radiative and nonradiative processes, respectively. This diagram does not represent all states involved in the mechanisms or their actual energies but does show some of the experimentally observed and predicted emission and isomerization processes.

No isomerization occurred at -196 °C, whereas delayed emission involving singlet and triplet states was very efficient. The absence of isomerization was indicated when the absorption spectra showed no change in intensity with respect to the duration of exposure to irradiation.

Emission intensity decreased with increase in temperature until it was quenched completely at room temperature, whereas isomerization became fastest at room temperature. This direct competition between delayed emission and the photochemical isomerization strongly suggests a direct participation of triplet states in the isomerization. Participation of reactive triplets in isomerization is in accord with the results of a study on a similar molecule, the unsubstituted 2-benzylidene-4-butyrolactone by Baumann, Ming-ta-Sung, and Ullman (1968) who found that isomerization can proceed through triplet state sensitization. These triplets were postulated to possess $\pi \rightarrow \pi^*$ character. According to Wagner and Hammond (1968), the lowest triplets responsible for slow emission are often also responsible for the photochemical reaction. Finally, the rather high quantum yields in both directions of isomerization at room temperature suggest that other deactivating processes are not efficient.

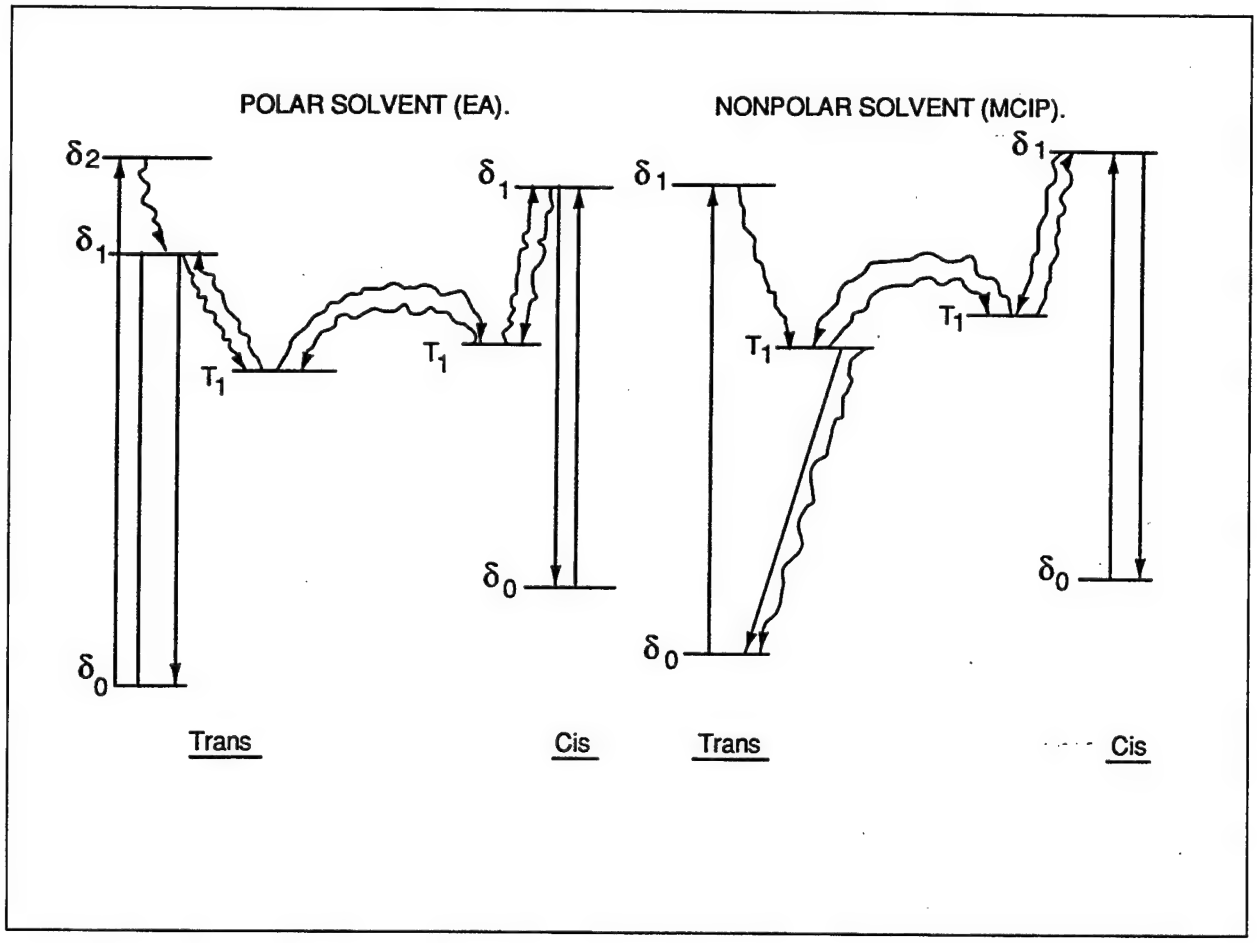

Figure 23. Jablonski diagram of polar/nonpolar solvent mechanisms

Using UV and VIS Spectra to Follow the Course of a Chemical Reaction

UV and VIS spectra can be used as an indication as to whether a new product has been formed and whether a reactant has totally disappeared. Consider the conjugation of Disperse Red 11: 1,4-diamine-2-methoxy-9, 10-anthraquinone and Disperse Blue 3: 1-[(2-hydroxyethyl)-amino]-9,10-anthra-quinone to bovine and guinea pig serum albumins, BSA and GPSA, respectively, to make the dye haptens large enough to be used as immunigens.

Figure 24 shows the UV and VIS spectra of the reactant, Disperse Red 11, Roman numeral I. on the graph; the conjugates of Disperse Red 11-BSA, numeral II.; and those of GPSA, represented by numeral III. The lines of the spectra represent various concentrations of each conjugate. The spectra of BSA conjugates appear to be identical to those of GPSA, and both are different from the spectra yielded by the pure dye.

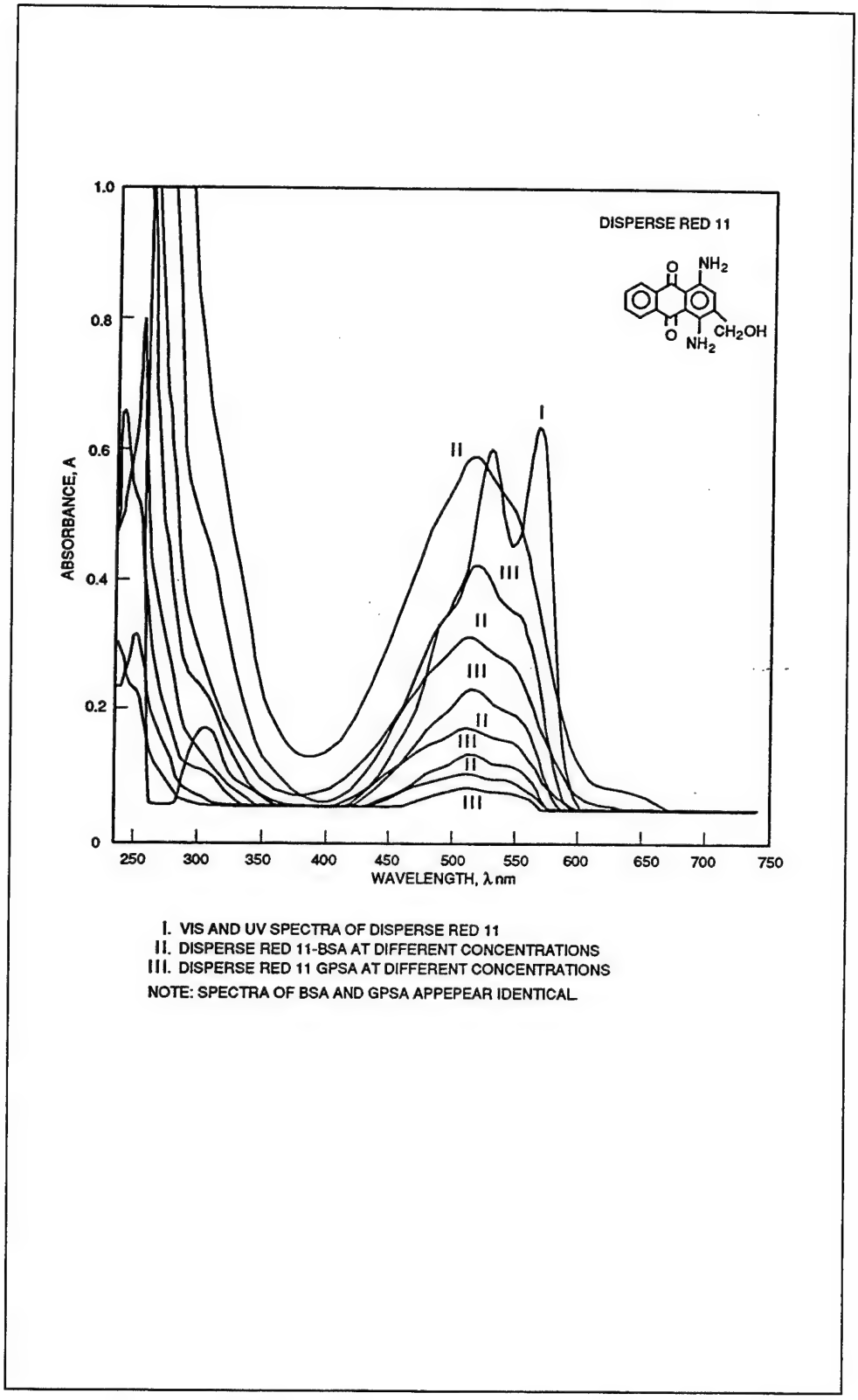

Figure 24. VIS and UV spectra of Disperse Red 11, BSA, and GPSA

UV and VIS spectra can also be used to monitor the course of separation and purification of organic compounds by separation techniques such as column chromatography (as discussed earlier). Figure 25 shows the spectra of four different fractions from a column chromatograph resulting from the conjugation of Disperse Blue 3 to BSA. Numeral I is a spectra of the first column chromatograph fraction of the unreacted dye. Numerals II and III are the spectra of the second and third fractions, from the column chromatograph, of the mixture of unreacted and protein conjugated dye. Numeral IV represents the spectra of the last fraction, which is due to the pure conjugated product alone.

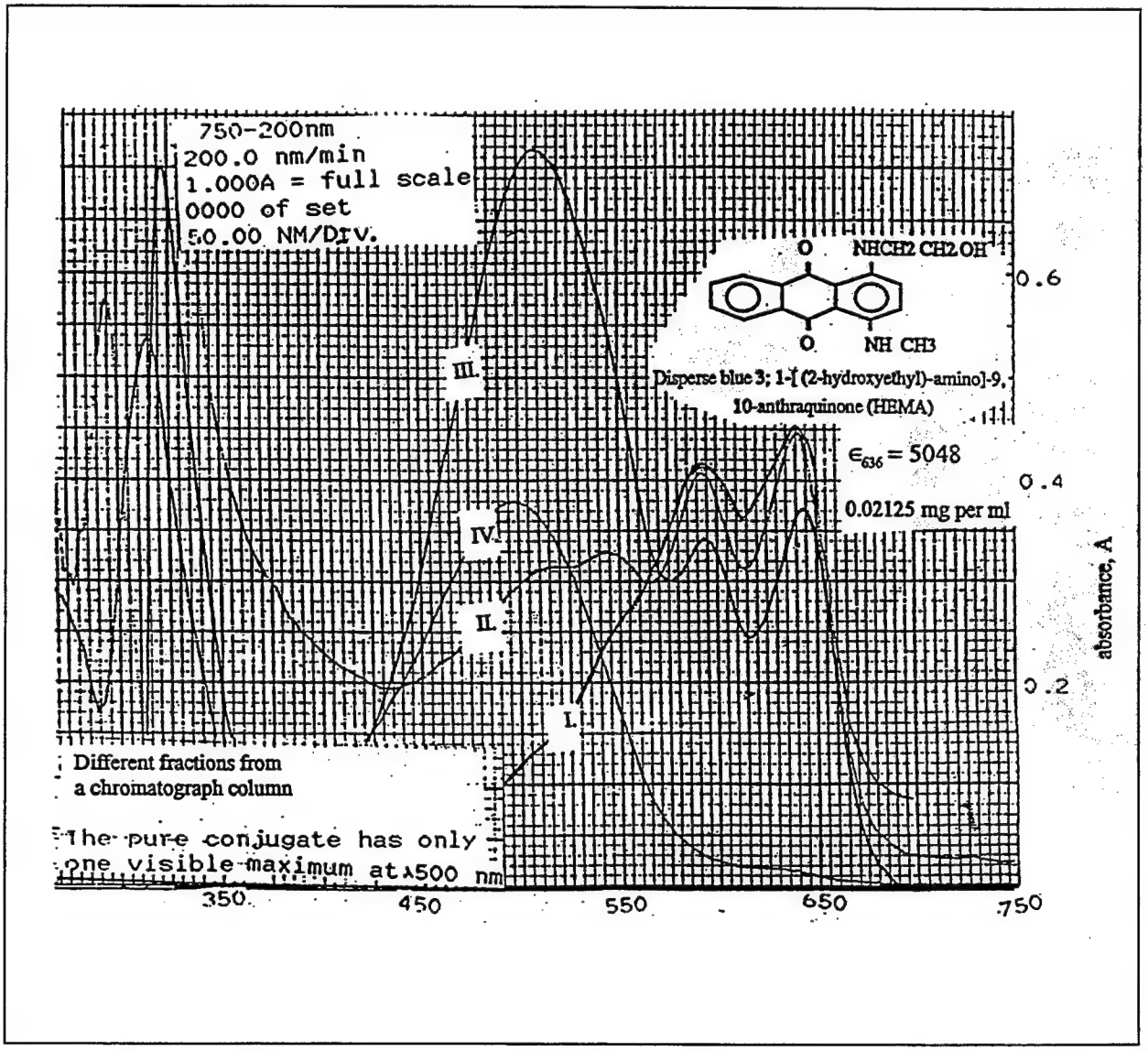

Figure 25. UV and VIS spectra showing the progression of a column chromatograph separation of unreacted Disperse Blue 3 from Disperse Blue 3-BSA conjugate

A photograph of a thin layer silica gel chromatogram corresponding to the above spectra confirms the course of purification (Figure 26).

Thus, it is shown that UV and VIS spectra, combined with other techniques, such as NMR and thin layer chromatography, can be a powerful means of the following the course of purification and identification.

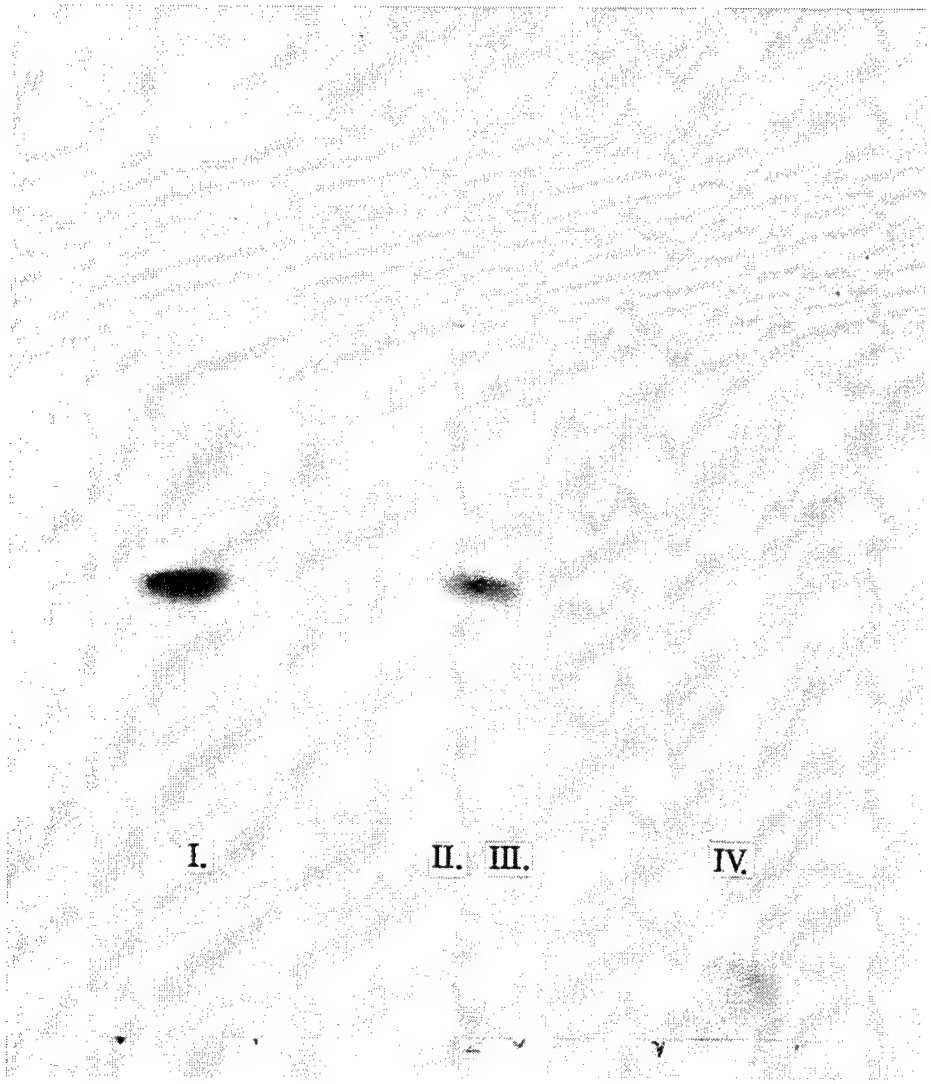

Figure 26. Photographs of TLC on plastic coated sheet

Use of a UV and VIS Stopped-Flow Technique for Reaction Rates Measurements and Optimization of an Analytical Assay

This technique is used for the study of rates of very fast reactions (10^{-3}s).

The stopped-flow spectrophotometer is a UV-VIS spectrophotometer that can follow fast signal changes in solutions because of its fast sampling system. Two reagents are placed into two syringes which can be driven instantaneously by a common push plate and discharged into a mixing chamber and into the observation cell. The sample volume is set by a stop syringe when its plunger is stopped suddenly by a rigid block thus triggering the data collection system. The stopped-flow spectrophotometer has two photodetectors, one for absorption changes (placed behind the cell window along the axis of the incident light) and another for emission changes (laced behind the cell window perpendicular to the first detector and to the incident beam). The theoretical basis for rate measurements and other detailed information about stopped-flow technique is given by Eccleston (1987), Gutfreud (1972), and Hiromi (1979).

Example of Use of Stopped-Flow Technique

Stopped-flow technique is used to optimize the UV/VIS spectrophotometric method for measuring hydrogen peroxide concentrations. This hydrogen peroxide assay is based on the classic iodometric method where hydrogen peroxide is reacted with excess potassium iodide (KI) to form iodine molecules (I_2) that in turn react instantaneously with I^- ions to form the complex ions I_3^-, according to the following equations:

$$2I^- + 2H^+ + H_2O_2 = I_2 + 2H_2O \quad \text{(slow reaction)} \tag{47}$$

$$I^- + I_2 = I_3^- \quad \text{(fast reaction)} \tag{48}$$

The I_3^- complex ion has a characteristic absorption spectrum with maxima at 290 and 360 nm. It is noteworthy that these same two absorption maxima were independently obtained when dilute solutions of known concentrations, made from iodine molecules (I_2) crystals, were reacted with excess potassium iodide (10 percent KI solution).

The absorbances at 290 and 350 nm (also at 560 nm when 24 percent starch solution was used as an indicator) showed direct proportionality or linear Beer's Law relationships to hydrogen peroxide concentrations when potassium iodide was used in excess. The absorption maxima for I^- and I_2 are at about 210 and 450 nm, respectively. Therefore, these absorption bands will not interfere with the assay, if freshly prepared iodide is used.

Stopped-flow technique was used to determine the rates of the above two reactions and to optimize the conditions of this hydrogen peroxide assay by making hydrogen peroxide or potassium iodide, one at a time, as the limiting reagent (100 ppm) while varying the concentrations of the other. It was found that the reaction is first order with respect to both reactants, H_2O_2 and KI (Figure 28). When a 10 percent KI concentration was used, a period of 20 seconds is needed to bring this reaction to completion (Figure 27). The rates of the slow and fast steps of the reaction are shown in Figure 28.

Conclusion

To summarize, it can be seen that spectroscopic techniques provide powerful tools to study:

a. Concentration changes.

b. Solvent effects.

c. Elucidation of excited states of some molecules.

d. Trends in UV and VIS spectral changes (wavelengths, molar absorptivities) due to structural changes such as adding electron donating or withdrawing groups to aromatic compounds or to the extension of the pi system conjugation.

e. The course of certain organic chemical reactions, such as in *cis-trans* isomerization or protein dye conjugation.

f. Steps of separation and purification by other analytical procedures, such as column chromatography.

g. Use of UV and VIS stopped-flow technique for measurements of reaction rates to optimize analytical assays.

Although the discussion presented here about photochemistry and spectroscopy is brief, this presentation may be useful to those who are interested in or who will be using these spectroscopic techniques.

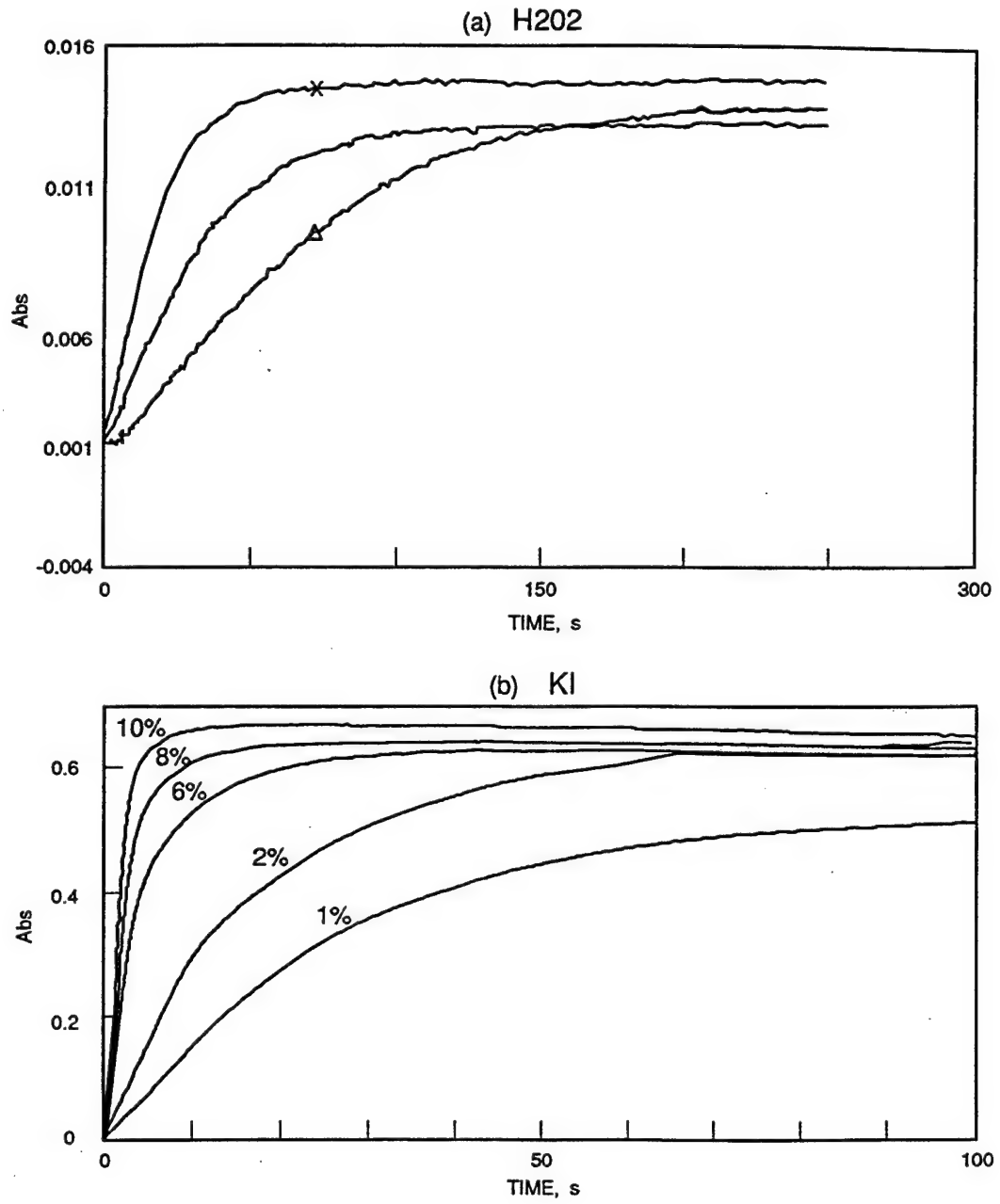

(a) Hydrogen Peroxide is variable: 500, 1,000, 2,000 ppm
Potassium Iodide is limiting reagent, 100 ppm
(b) Potassium Iodide is variable: Hydrogen Peroxide is 100 ppm

Figure 27. Absorbance rates of H_2O_2 and KI reactions at 350 nm

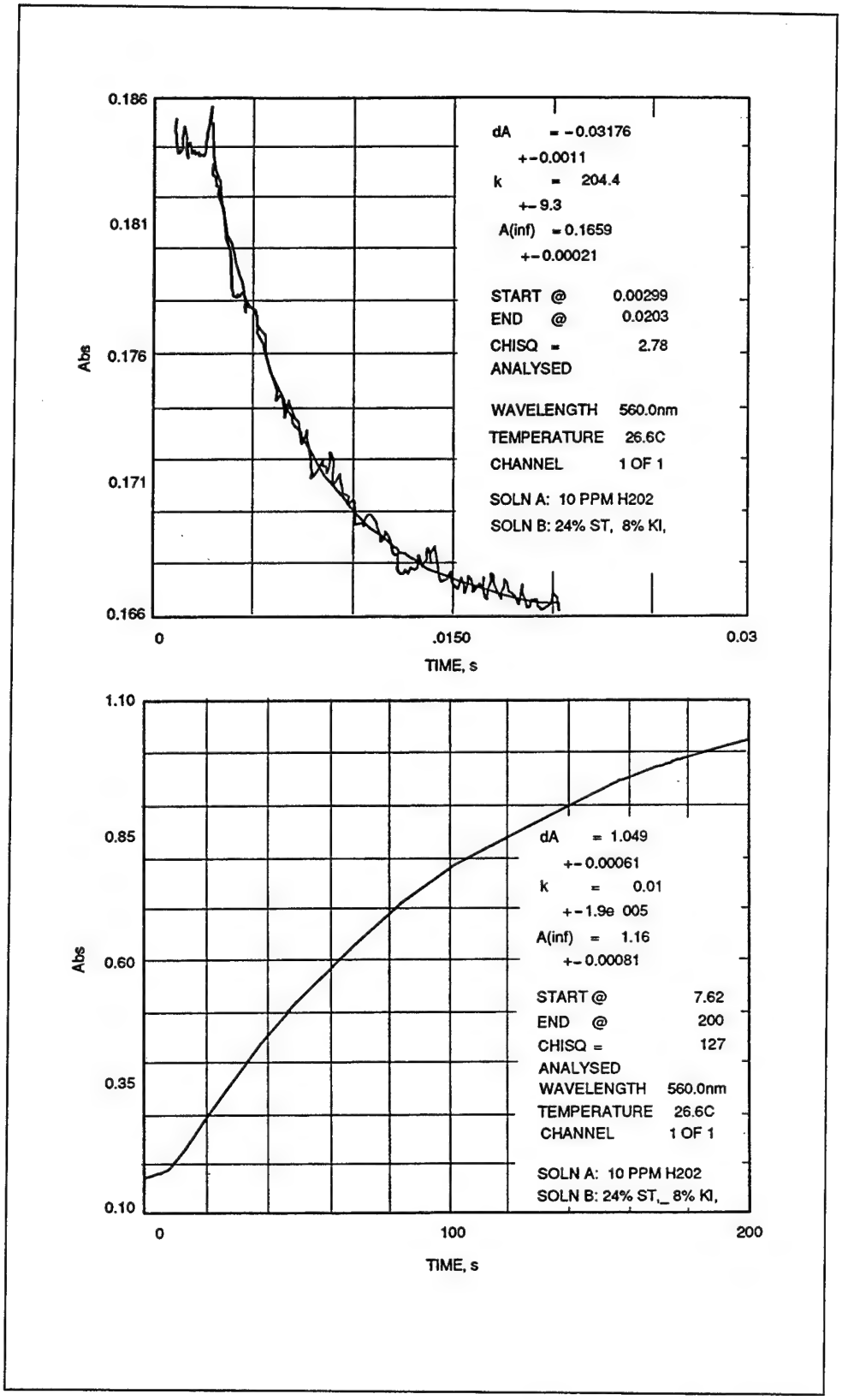

Figure 28. Rates of a fast and slow two-step reaction of H_2O_2 with excess iodide ions

Useful Constants

Atomic Mass Unit	$M_u = 1.66056555*10^{-27}$ kg
Avogadro Constant	$N = 6.0221367*10^{23}$ mole^{-1}
Boltzmann Constant	$K = R/N = 1.38066*10^{-23}$ J K^{-1}
Charge to Mass Ratio	$e/m = 1.758796*10^{11}$ Coulomb kg^{-1}
Electronic Charge	$e = 1.60217733*10^{-19}$ Coulomb
Electron Volt	$eV = 1.60217733*10^{-19}$ J
Planck's Constant	$h = 6.62620755*10^{-34}$ Js $h = h/2\pi = 1.054887*10^{-34}$ Js
1 Electron Volt/Planck's Constant	$1eV/h = 2.4179696*1014$ H
Rest mass of electrons	$M_e = 9.1093893*10^{-3}$ kg $= 5.485712*10^{-4}$ amu
Rest mass of neutron	$M_n = 1.6749286*10^{-27}$ kg $= 1.008665$ amu
Rest mass of proton	$M_p = 1.672623*10^{-27}$ kg $= 1.00727605$ amu
Rydberg Constant for Hydrogen Atom	$R_H = 2.1798741*10^{-18}$ J
Universal Gas Constant	$R = 8.31441$J K^{-1}mole^{-1} $= 1.987216$ cal K^{-1}mole^{-1} $= 8.314510*10^{-2}$bar K^{-1}mole^{-1} $= 8.2057*10^{-2}$l atm K^{-1}mole^{-1}
Speed of Light in Vacuum	$C = 2.99792458$ ms^{-1}

References

Alberty, R. A. (1983). *Physical chemistry*. 6th ed., Wiley, New York.

Atkins, P. W. (1990). *Physical chemistry*. 4th ed., Freeman, New York, 292.

Barrows, G. (1981). *Physical chemistry for life science*. McGraw-Hill, New York.

Baumann, N., Ming-ta-Sung, Ullman, E. F. (1968). *J. Am. Chem. Soc.* 909, 4157-8.

Bromberg, J. P. (1980). *Physical chemistry*. Allyn and Bacon, Boston, 533-535.

Ebbing, D. D., Wrighton, M. S. (1990). *General chemistry*. Houghton Mifflin, Boston.

Eccleston, J. F. (1987). *Stopped-flow spectrophotometric techniques 6*. IRL Press.

Fessenden, R. J., and Joan, S. (1982). *Organic chemistry*, 1st ed., Willard Grand Press, Boston.

Gillespie, A. M., Jr. (1985). *A manual of fluorometric and spectrophotometric experiments*. Gordon and Breach Science Publishers, S. A., New York.

Gutfreud, H. (1972). *Enzymes: Physical principles*. Wiley-Intescience, London, England.

Hiromi, K. (1979). *Kinetics of fast enzyme reactions*. Wiley, New York.

Levine, I. N. (1983). *Physical chemistry*. McGraw-Hill, New York.

Parker, C. A. (1966). "Organic trace analysis by fluorescence and phosphorescence measurements." *Proceedings of the Royal Society*. 108-109.

Wagner, P., and Hammond, G. (1968). *Advances in photochemistry 5*, 21.

Bibliography

Denney, R. C., and Sinclair, R. (1991). "Visible and ultraviolet spectroscopy." *Analytical chemistry*. Open Learning series. Wiley, New York.

Ege, S. (1989). *Organic chemistry*. Heath, Lexington, MA.

Handbook of Chemistry and Physics. (1979). 60th ed., CRC Press.

Jaffe, H. H., and Orchin, M. (1962). *Theory and applications of ultraviolet spectroscopy*. Wiley, New York.

Jenkins, T. F. (1990). "*Development of a simplified field method for the determination of TNT in soil*," Special report 90-38, U.S. Army Engineer Waterways Experiment Station, Vicksburg, MS.

Parker, C. A. (1958). "Direct recording of fluorescence excitation spectra," *Nature* 182(4641), 1002-04.

_____. (1968). "Photoluminescence analysis." *Proceedings of the Royal Society*. 76.

Parker, C. A., et al. (1962). "The possibilities of phosphorescence measurement in chemical analysis: Tests with a new instrument." *The Analyst* 87, 664.

_____. (1962). "Sensitized anti-stokes delayed fluorescence." *Proceedings of the Royal Society*. 386.

_____. (1965). "Sensitized delayed fluorescence as an analytical method." *The Analyst* 90(1066), 1-8.

Qasim, M. (1964). *Photocatalytic properties of zinc oxide in oxidation reactions*. M.S. thesis, Bowling Green State University, Bowling Green, OH.

_____. (1968). *Cis-trans photoisomerization of 2-(p-dimethylaminobenzulidene)-4-butyrolactone*. Ph.D. diss., University of Cincinnati, Cincinnati, OH.

Solomons, T. W. G. (1988). *Organic chemistry*, 4th ed., Wiley, New York, 570-573.

Streitwieser, A., Heathcock, C. H., and Kosower, E. M. (1992). *Introduction to organic chemistry*. Macmillan, New York, 670-673, 679.

Williamson, K. L. (1989). *Macroscale and microscale*. Heath, Lexington, MA, 59-265.

REPORT DOCUMENTATION PAGE

Form Approved
OMB No. 0704-0188

1. AGENCY USE ONLY *(Leave blank)*	2. REPORT DATE	3. REPORT TYPE AND DATES COVERED
	April 1997	Final report

4. TITLE AND SUBTITLE
Simplified Concepts in Spectroscopy and Photochemistry

5. FUNDING NUMBERS

6. AUTHOR(S)
Mohammed Qasim

7. PERFORMING ORGANIZATION NAME(S) AND ADDRESS(ES)
U.S. Army Engineer Waterways Experiment Station
3909 Halls Ferry Road
Vicksburg, MS 39180-6199

8. PERFORMING ORGANIZATION REPORT NUMBER
Technical Report IRRP-97-3

9. SPONSORING/MONITORING AGENCY NAME(S) AND ADDRESS(ES)
U.S. Army Corps of Engineers
Washington, DC 20314-1000

10. SPONSORING/MONITORING AGENCY REPORT NUMBER

11. SUPPLEMENTARY NOTES
Available from National Technical Information Service, 5285 Port Royal Road, Springfield, VA 22161.

12a. DISTRIBUTION/AVAILABILITY STATEMENT
Approved for public release; distribution is unlimited.

12b. DISTRIBUTION CODE

13. ABSTRACT ***(Maximum 200 words)***

Spectrophotometric techniques are powerful tools for determining both qualitative (including structural) and quantitative changes in organic and inorganic compounds, and these techniques are particularly useful for studying: concentration changes; solvent effects; the excited states of certain molecules; trends in ultraviolet (UV) and visible (VIS) spectral changes (due to such structural changes as the addition of electron donating or withdrawing groups to aromatic compounds or to the extension of pi system conjugation); the course of certain organic chemical reactions (such as in *cis-trans* isomerization or protein dye conjugation); steps in separation and purification by other analytical procedures (such as column chromatography); and use of UV and VIS stopped-flow technique for measurements of reaction rates in the optimization of analytical assays.

This paper attempts to provide sufficient discussion of theoretical concepts for practical applications of spectroscopy and photochemistry to be more easily understood. However, the emphasis is on practical application, particularly through showing representative uses and examples of UV and VIS techniques with organic molecules.

14. SUBJECT TERMS	15. NUMBER OF PAGES
See reverse.	84
	16. PRICE CODE

17. SECURITY CLASSIFICATION OF REPORT	18. SECURITY CLASSIFICATION OF THIS PAGE	19. SECURITY CLASSIFICATION OF ABSTRACT	20. LIMITATION OF ABSTRACT
UNCLASSIFIED	UNCLASSIFIED		

14. Subject Terms.

Applications--UV, VIS spectra--study organic molecules--emission spectra--study excited states--follow course of chemical reaction--UV, VIS stopped-flow;
Basic concepts;
Basic tools--Lambert-Beer law--spectrophotometers--UV--VIS--IR--absorption--emission--monochromator--lasers
Regions of electromagnetic radiation--X-rays--UV--VIS--singlet, triplet electronic excited states--fluorescence--phosphorescence--quantum yield--pi, sigma electrons
Structural molecular changes and UV, VIS wavelength, molar absorptivity--solvents-conjugation of polyenes--carbonyl groups--methyl substitution--polycyclic aromatic compounds--interactions n, π electrons--benzene ring--methyl, chloro substitutions--di-;trinitrobenzenes, toluenes
Vibrational, rotational excitations--IR--FTIR--microwave--NMR--Raman spectra

Destroy this report when no longer needed. Do not return it to the originator.